NOAA Technical Report ERL 416-AOML 31

Electrical Resistivity/Conductivity of Submarine Sediments Measured by In Situ Techniques

Matthew H. Hulbert
Douglas N. Lambert
Richard H. Bennett
G. L. Freeland
John T. Burns
W. B. Sawyer

December 1981

U.S. DEPARTMENT OF COMMERCE
National Oceanic and Atmospheric Administration
Environmental Research Laboratories

NOAA Technical Report ERL 416-AOML 31

Electrical Resistivity/Conductivity of Submarine Sediments Measured by In Situ Techniques

Matthew H. Hulbert
Douglas N. Lambert
Richard H. Bennett
G. L. Freeland
John T. Burns
W. B. Sawyer

Atlantic Oceanographic and Meteorological Laboratories
Miami, Florida

December 1981

U.S. Department of Commerce
Malcolm Baldrige, Secretary

National Oceanic and Atmospheric Administration
John V. Byrne, Administrator

Environmental Research Laboratories
Boulder, Colorado
George H. Ludwig, Director

NOTICE

Mention of a commercial company or product does not constitute an endorsement by NOAA Environmental Research Laboratories. Use for publicity or advertising purposes of information from this publication concerning proprietary products or the tests of such products is not authorized.

CONTENTS

ABSTRACT. An in situ four-electrode contact resistivity probe system was designed, fabricated, and field tested for use in coarse-grained carbonate sediments. The probe was designed to be driven to selected depths below the seafloor using a standard Vibracore system. The probe tip was machined from 5-in-diameter polycarbonate plastic, which has high impact, tensile, and compressive strengths and a high volume resistivity of 10^{16} ohm/cm. The electrodes were fabricated from ¼-in-diameter, hardened tool steel and tapered to a point (25° angle) to provide a consistent surface area. The probe tip was machined to form a wedge for ease of insertion into the seafloor. The four insulated electrodes, spaced equidistant across the wedge, were extended beyond the probe tip to minimize effects of sediment disturbance by the wedge insertion. In situ measurements of resistivity were recorded on board ship by precision electronic equipment consisting of signal generators and processors, and by temperature-monitoring systems, which were hard-wired to the probe. Solutions of different known salinities were used to calibrate the entire probe system prior to and after field measurements. Overall limits of uncertainty at respective depths below the seafloor range between ±2 and ±15 percent of the measured values. Best estimates of conductivity are considered to be ±3 percent of the reported values. Resistivity measurements were made at six sites in carbonate sediments off South Florida to a maximum depth of penetration of ~17 feet. Average values of conductivity ranged between 0.88 and 1.21 mho/m. The seabed was found to be composed of alternating layers of relatively high-conductivity material (0.8 to 1.4 mho/m) in thicknesses of a few feet and layers about 1-ft thick having relatively low conductivities in the range of 0.4 to 0.8 mho/m.

ELECTRICAL RESISTIVITY/CONDUCTIVITY OF SUBMARINE SEDIMENTS MEASURED BY IN SITU TECHNIQUES

M. H. Hulbert[1], D. N. Lambert, R. H. Bennett,
G. L. Freeland, J. T. Burns, W. B. Sawyer[2]

1. INTRODUCTION

To develop an understanding of the detailed electrical properties of the seabed, one of the necessary parameters is the electrical conductivity (or its reciprocal, the resistivity). An in situ system capable of obtaining in situ conductivities of surficial sediments would be expected to provide critical data leading to the determination of porosity and wet bulk density of not only cohesive sediments but also sand deposits (predominantly quartz grains) and coarse-grained carbonates. The determination of the geotechnical properties of undisturbed, noncohesive sediments is an area of much-needed research. Advances in technology would add an important dimension to scientific and engineering knowledge and capabilities in the study of the properties of surficial sediments. Density and porosity data are fundamental information required in the study of sedimentary diagenesis, pore fluid migration, and consolidation history, and in numerous engineering applications.

Resistivity measurements have a long history of successful use in geophysical surveying and in exploration for petroleum and other minerals (Pirson, 1963; Wyllie, 1963; Griffiths and King, 1965; Keller and Frischknecht, 1966; Parkhomenko, 1967; Ginzburg, 1974; Dobrin, 1976). Despite this, the measurement of electrical conductivity in unconsolidated submarine sediments, to the desired accuracy of ±10 percent and with a vertical resolution of approximately 25 cm, presents a challenge (Kermabon et al., 1969; Sweet, 1972; Erchul, 1974; Jackson, 1975).

2. GEOLOGY AND MORPHOLOGY OF THE STUDY AREA

The study area is located on the Florida continental shelf off Fort Lauderdale in the northern Straits of Florida, through which the warm waters of the Gulf Stream pass northward into the Atlantic Ocean (fig. 1). The narrow Florida shelf (approximately 2.8 km) is bounded by the shoreline to the west and generally the 21-m bathymetric contour to the east. The seafloor gradient then steepens down to the broad Miami Terrace in water depths of 220 to 366 m (Siegel, 1959). The shelf in this area is characterized by a series of three reef ridges running roughly north-south parallel to the shoreline (fig. 2). These ridges form highs between a series of steplike linear flats or plateaus (fig. 3). The reefs are composed of hard substrate, and the lows are depressions partially filled with white to gray unconsolidated calcareous sands and gravels.

---

[1]International Minerals and Chemical Corp., Terre Haute, Indiana
[2]U. of Texas, Inst. for Geophysics, Galveston, Texas

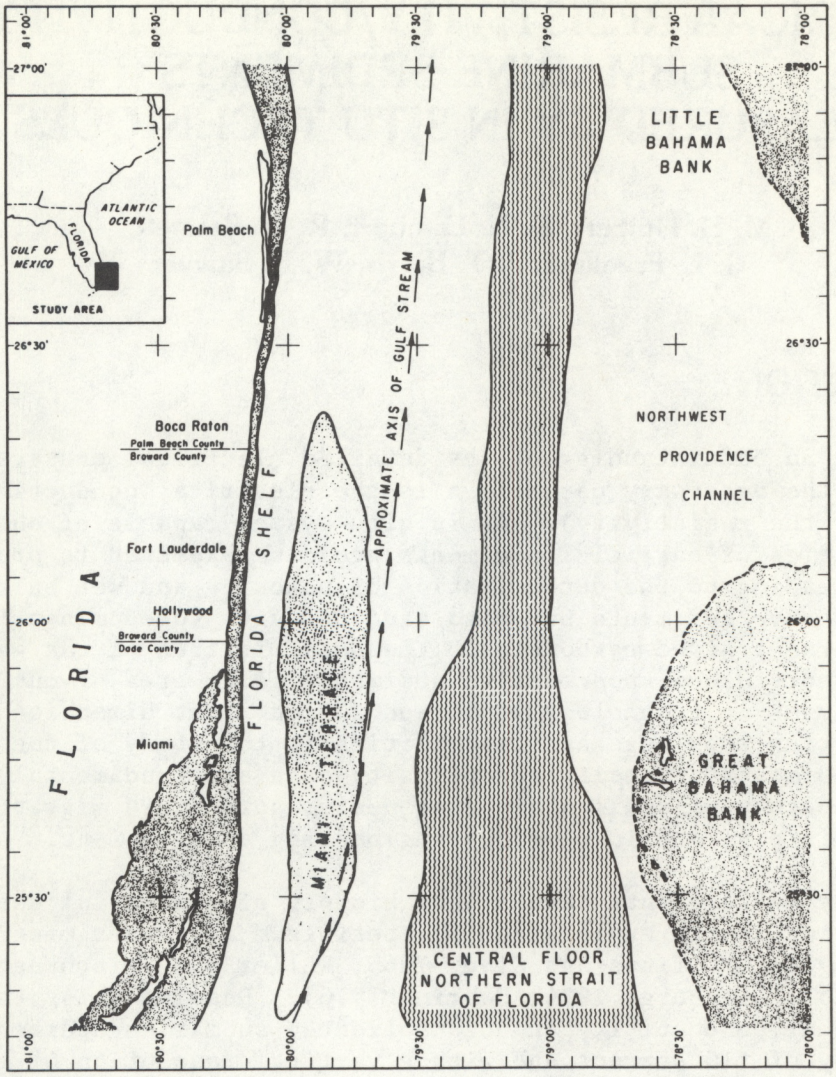

Figure 1.--Physiographic provinces of the northern Straits of Florida (Duane and Meisburger, 1969).

The outer or third reef is a relic barrier reef that flourished during the early Holocene sea level transgression. Acropora palmata was the dominant reef framework builder during this reef's formation. Lighty et al. (1978) postulate that the rapid flooding of the continental shelf may have caused periods of extensive turbidity and temperature fluctuations that brought about the decline of the Acropora palmata approximately 7,000 years ago. This shallow-water, early-Holocene barrier reef has been highly altered and masked by a lithified crust produced by epifauna of deeper waters. Present-day fauna on its surface includes alcyonarians, sponges, and scattered coral heads (Lighty et al., 1978). The reef crest is highly irregular at a depth of approximately 15 m and has a typical relief of 3 to 5 m.

The middle or second reef is a linear, continuous substrate with an irregular surface averaging approximately 12 m below sea level. Using information from a dredge cut, Shinn et al. (1977) have described the reef

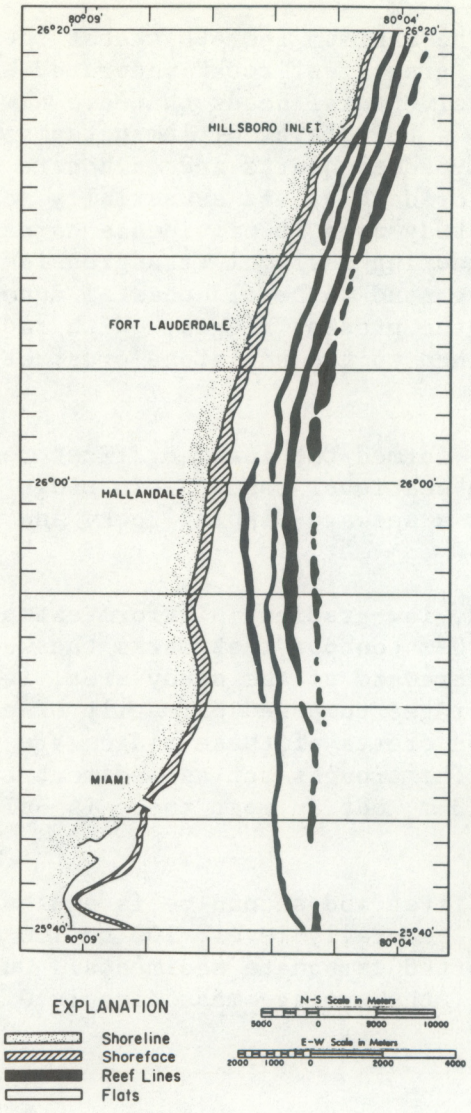

Figure 2.--Southeastern Florida continental shelf morphology. Locations of the north-south trending reefs are indicated (after Duane and Meisburger, 1969).

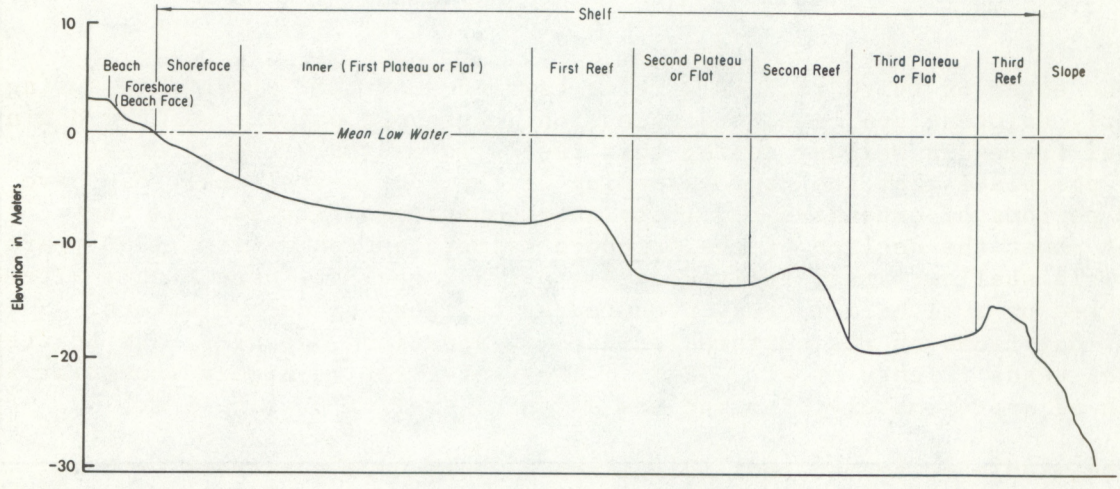

Figure 3.--Schematic profile of southeastern Florida shore and shelf morphology (after Duane and Meisburger, 1969).

several miles south of the study area. The maximum reef thickness there is 2.4 m. It is composed of extremely hard, gray "reef rock" indurated by extensive alteration and infilling of massive coral heads that are now nearly unidentifiable. Below the "reef rock" is a thin layer of laminated soilstone crust overlying a lightly cemented, cross-bedded quartz and carbonate sand. A similar soilstone crust found in the Florida Keys was subaerially formed (Multer and Hoffmeister, 1968). In the study area it provided a hard substrate onto which the corals attached initially during sealevel transgression. Shinn et al. (1977) believe the underlying sand to be old coastal dunes that controlled the location and linearity of the present ridges. With radiocarbon they dated a single unaltered coral attached to the soilstone crust at 6,300 ± 120 years.

A similar process is thought to have formed the inner or first reef, although at a slightly later time, as the sea level rose. This ridge occurs at approximately the 10-m contour and has a seaward-dipping rocky and irregular face with 3 to 5 m of relief.

The inner flat or plateau is a broad, low-gradient platform extending from the shoreline to approximately the 10-m contour that marks the western edge of the first reef. This plateau, shoreward of the study area, is characterized by low-relief linear swales and ridges composed primarily of coquina limestone of the Anastasia formation. The crests of these ridges are usually encrusted by reef-associated organisms. The troughs act as sediment traps, and in places sediment thickness exceeds 3 m, but in most there is only a thin cover (Raymond, 1972).

The second plateau lies between the first and second reefs and has a depth ranging between 11 and 14 m. It is generally level, 100 to 150 m wide, and composed of unconsolidated, poorly sorted carbonate sediments. Quartz content is typically less than 10 percent; the average mean size is 0.62 mm (Raymond, 1972).

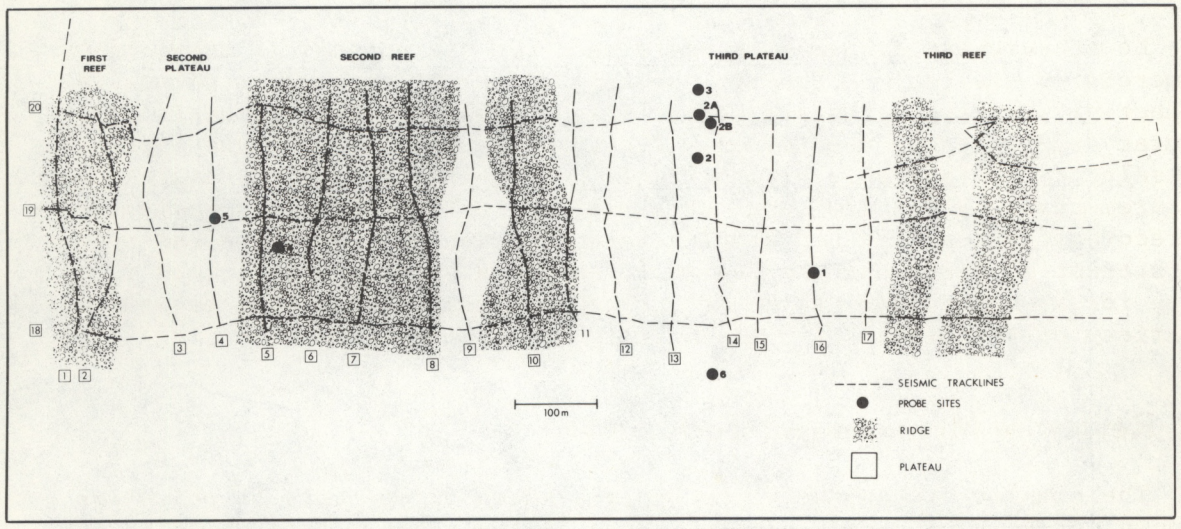

Figure 4.--Map of the study area, showing the location of the seismic tracklines and resistivity probe sites.

The majority of resistivity probe measurements were collected in the third plateau, which is located between the second and third reefs (fig. 4). This trough is approximately 400 m wide in the study area and is filled with 6 to 8 m of carbonate sand and reef rubble, most of which is unconsolidated. Its floor varies in depth from 18 to 21 m. The greater depths near the second reef give the floor a slight shoreward dip. Sediments found in this low area are primarily medium carbonate sands with large amounts of gravel-sized to cobble-sized reef debris interspersed. Mean size of the sand fraction is 0.47 mm with a low quartz concentration, typically <15 percent (Raymond, 1972). Duane and Meisburger (1969) have reported that the acid-soluble content of this inter-reef sediment is generally 80 percent.

3. MEASUREMENT SYSTEMS

3.1 Concepts

The goal is to measure electrical resistivity/conductivity in unconsolidated marine sediments, with accuracy of ±10 percent and a vertical resolution of ~0.3 m. That presents a challenge despite the long history of electrical-resistivity measurements in geophysical surveying and oil exploration. Laboratory measurement of conductivity requires recovery of the sediment in a condition sufficiently undisturbed that the conductivity is the same (within the prescribed accuracy) as when the sediment is in place; in situ measurement with the desired resolution appears to require that the measuring device itself be emplaced within the sediment. Recovery of sufficiently undisturbed sediment samples should be possible in fine-grained deposits (muds), but recovery of undisturbed samples in coarse sand materials, such as the carbonate debris at the study site, is unlikely. For accuracy goals to be met with in situ measurement, the volume of sediment disturbed by device emplacements needs to be small compared with the volume of sediment responding to electrical input--a need somewhat in conflict with that imposed by the resolution requirement, which demands that the vertical extent of the sediment response be minimized.

No measurement system that could meet the stated goal is known to be commercially available. However, several different approaches to making conductivity measurements are potentially capable of yielding satisfactory accuracy and vertical resolution. The most appropriate of these approaches was selected on the basis of additional goals, in particular, completing the measurements within a few weeks at a minimal cost. Laboratory measurements on recovered unconsolidated samples were rejected for use since the sediment of interest is sandy and the degree of sample disturbance is likely to be too large for accuracy goals to be met. In-place measurements can be made using a variety of techniques that are briefly discussed below.

3.2 Review of Measurement Techniques

The simplest technique is to apply a known direct-current potential (or a known current) to a pair of electrodes having a known separation in the sediment, and to measure the resulting current flow (or the potential) between the electrodes. Application of Ohm's Law yields the apparent resistance from which the apparent resistivity and the apparent conductivity can be calculated.

(Resistivity of a material is the electrical resistance of a cylinder of the material having unit length and cross-sectional area; conductivity is the reciprocal of resistivity.) The two-electrode direct-current technique has the advantage of requiring a minimum of apparatus and can therefore be made into an operational system relatively cheaply and quickly. It suffers from two severe drawbacks: (1) In addition to the electrical resistance of the sediment itself, there is a contribution to the apparent resistivity due to electrochemical, or polarization, resistance, and (2) the current density in the near vicinity of each of the electrodes is very high so that contact resistance at the electrodes can be a major contributor to the apparent resistivity. The contribution to the resistance resulting from electrochemical reactions can be minimized by using alternating current rather than direct current. There is a slight increase in cost and complexity. The effect of contact resistance can be minimized by using two pairs of electrodes, one for applying a known current and the other for measuring the resulting electrical potential (Keller and Frischknecht, 1966). In submarine environments, the potentials to be measured for both the two-electrode and four-electrode techniques are quite small; therefore, sensitive electronic instrumentation (most of which is commercially available) is required to detect the signal and discriminate against noise. In addition, emplacement of the electrodes is difficult, especially in sandy sediments, because (1) firm electrode contact with the sediment must be maintained, (2) free communication with the overlying, highly conductive seawater must be avoided, and (3) electrode arrays tend to be somewhat fragile; they must be designed with electrode spacing less than 40 percent of desired resolution and electrode size sufficiently small to minimize sediment disturbance.

These emplacement problems can be substantially reduced by using an inductive technique rather than contact electrodes, but for the complex device required, development time is long and cost is high (Dobrin, 1976). Inductive techniques rely upon detection of the secondary electromagnetic field established in conductive materials by an applied electromagnetic field. The field to be applied is produced by an alternating current flowing in a loop or coil of wire; no physical contact is required between the material being studied and either the primary (transmitter) coil or the secondary (receiver) coil. For both contact and inductive techniques, the vertical extent of the sediment contributing to the resistivity measurement can be controlled to a substantial degree by the addition of guard electrodes or coils to which is applied an appropriate electrical waveform, but again the equipment is costly and complex (Sweet, 1972).

3.3 Choice of Methodology and Design of Systems

The system selected to achieve the measurement goals was based on the four-electrode contact technique. The device took the form of a probe (fig. 5) at the tip of a Vibracore pipe. The probe is wedge shaped to ease emplacement and minimize sediment disturbance, and is fabricated of nonconductive plastic (see sec. 3.3.1). The electrodes extend beyond the wedge and are spaced so that (1) the total volume of sediment that contributes to the resistivity measurement is large compared with the portion of the volume that has been disturbed, (2) the vertical resolution of the measured resistivity is adequate, and (3) the electrode separation is at least three times the expected grain size of the sediment (Parkhomenko, 1967). The electrodes are equally spaced with the two potential-measuring electrodes on the inside, in the "Wenner

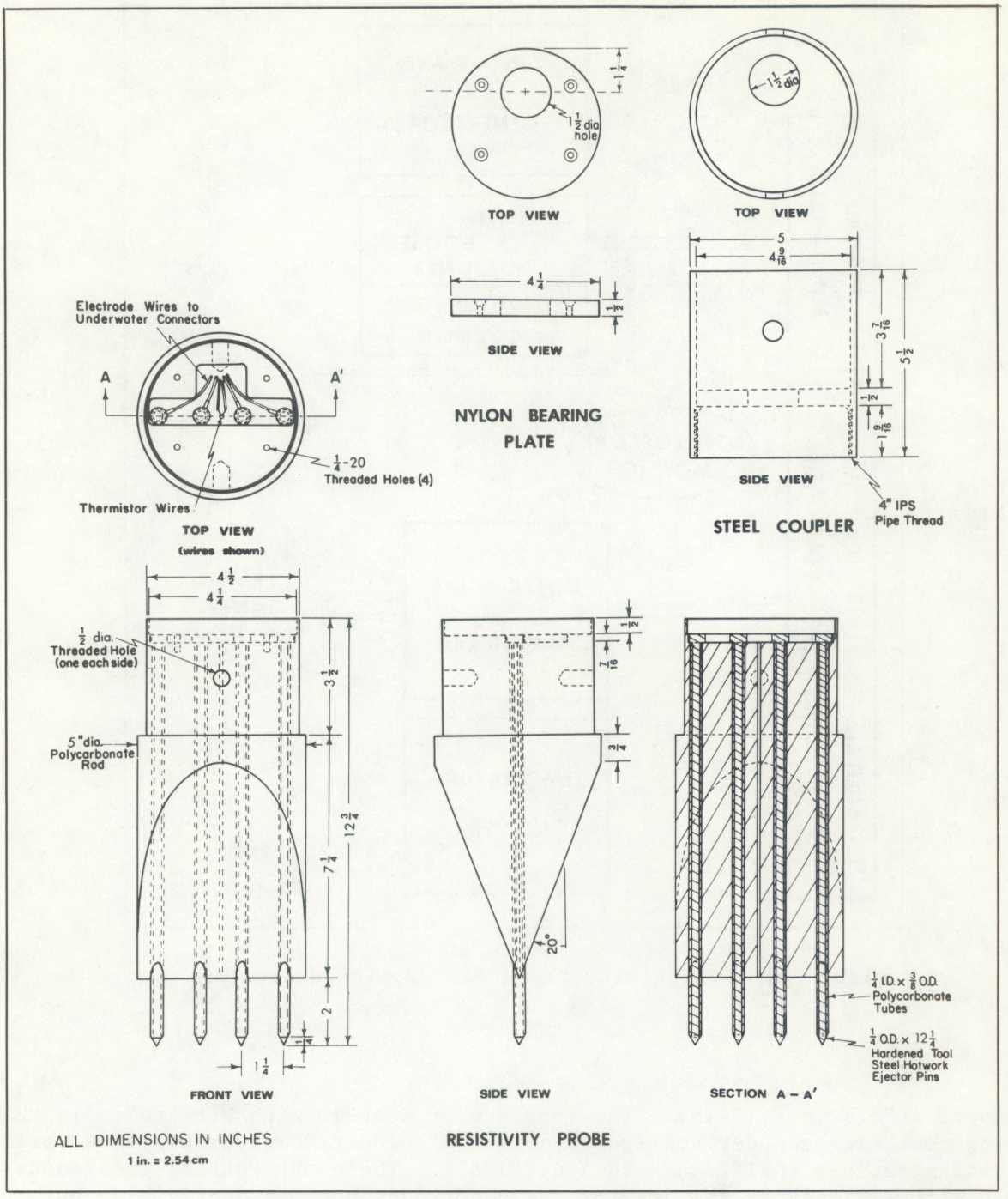

Figure 5.--Mechanical drawing of resistivity probe and components.

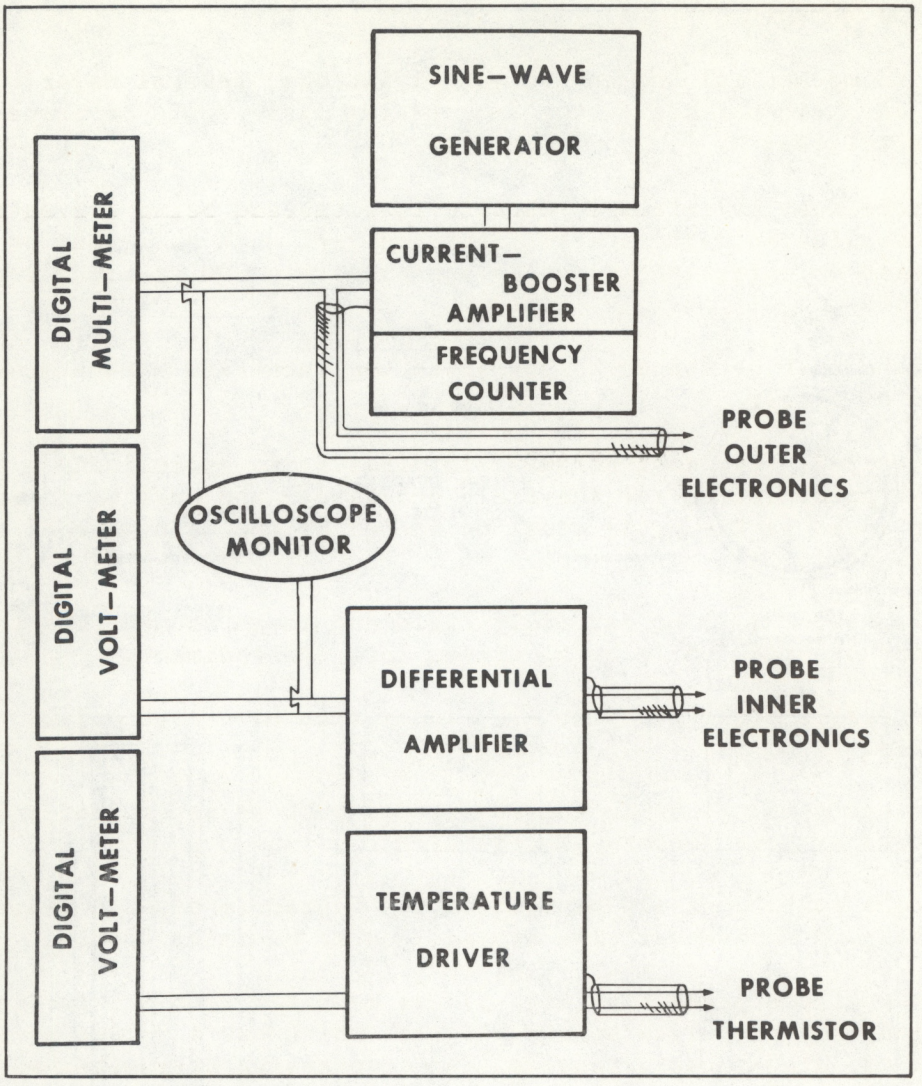

Figure 6.--Resistivity probe electronics subsystem.

arrangement" (Wenner, 1915). The response of systems with electrodes in this arrangement has been derived from theory for conductive materials in a variety of configurations (Griffiths and King, 1965). These theoretical treatments apply strictly only as the area of the electrodes becomes negligible, but the limiting cases are useful in understanding the behavior of real electrode systems.

Alternating current is supplied at up to approximately 20 volts to the outer electrodes. The inner, potential-measuring electrodes are connected to a unity-gain differential amplifier with a high common-mode rejection ratio and a high-input impedance; output of the amplifier and the current source are monitored. Temperature at the probe tip is monitored with a thermistor circuit since the sediment resistivity varies 1.5 percent per degree Celsius (Boyce, 1967). All connections to the probe are made by means of two-conductor shield cable. A block diagram of the electrode instrumentation is shown in fig. 6.

3.3.1 Physical System

Owing to mechanical and environmental factors, several major considerations were taken into account before the resistivity probe could be properly developed. They are as follows:

(1) The probe must be extremely durable to withstand being driven through semiconsolidated carbonate sediment and reef rock materials by a Vibracore with an effective weight of approximately 360 kg and a high rate of vibration.

(2) The probe must be shaped to penetrate the substrate with a minimum amount of effort.

(3) The electrode tips must be small in diameter to approximate a theoretical point source for the field generated, and must be located far enough ahead of the probe wedge to be out of the main zone of sediment disturbance.

(4) The electrodes must be extremely rigid and tough enough that they will not bend or erode while being driven into the sediment.

(5) All materials other than the electrodes must have high volume resistivities.

(6) Electrical connections to the electrodes must be waterproof and able to withstand extreme amounts of vibration.

(7) The probe must be easily mounted on the Vibracore pipe to minimize assembly and changeover time at sea, and to minimize cost.

The body of the probe tip (fig. 5) was machined from a 5-in-diameter by 12 3/4-in-long rod of polycarbonate plastic, which has a volume resistivity of 10^{16} ohm-cm; high-impact, tensile, and compressive strengths; and low water absorption. It also has excellent machining characteristics. Four holes with 9.5-mm (3/8-in) diameter were bored in a straight line 31.8 mm (1¼ in) apart, the length of the rod. A recess was cut into the top of the rod to accept a 12.7-mm (½-in)-thick by 108-mm (4¼-in)-diameter nylon bearing plate which rests on top of the electrode heads. An 11.1-mm (7/16-in) channel was machined into the recess to accept the electrode heads and electrical wires.

A 20° angle was machined on two sides of the rod to form a wedge-shaped leading edge to ease penetration into the sediments. The top 88.9 mm (3½-in) of the rod were turned down to 114.3-mm (4½-in) diameter to make a slip-fit inside the steel coupler. The rod was held in place inside the coupler by two threaded steel studs with 12.7-mm (½-in) diameter.

The electrodes were made from standard hardened tool-steel hotwork ejector pins, 6.4 mm (¼ in) in diameter. They were selected for their hardness and ability to withstand constant physical punishment. A tube of polycarbonate insulator (9.5 mm [3/8 in] outside diameter by 6.4 mm [¼ in] inside diameter) was cemented with solvent over the entire length of the steel rods. A point with an angle of 25° was then precision ground on each rod and insulator to ensure an equal amount of exposed surface area on each electrode tip.

Electrical wires were attached to the electrode heads by soldering them into a small piece of 3.2-mm (1/8-in)-diameter copper tubing that had been brazed into the rod head. The electrodes were then tapped into place in the polycarbonate wedge. A waterproof seal was assured by the use of silicone dielectric grease in the space between the electrode insulator and the wedge.

The bearing plate that held the electrodes in place (vertically) was machined of nylon chosen for its high volume resistivity (10^{13} ohm/cm) and superior compressive strength. Before assembly of the bearing plate, the wire channel and recess at the top of the polycarbonate wedge were filled with silicone grease. The nylon plate was then screwed down into place until it rested on top of the electrode heads. As it was screwed down, some of the silicone grease was squeezed out, filling all voids, thus assuring that the cavity around the electrode heads and wires was completely waterproofed.

This "soft potting" of the system was selected because of the difficulty of "hard potting" several different materials (polycarbonate, nylon, and neoprene wire insulation) and the probability that the large vibrating forces exerted on the materials would break down their waterproof integrity and thus cause electrical shorts across the electrodes. After assembly, all probe tips were pressure tested in a hyperbaric chamber to 0.69 MPa (100 psi) to check for water leakage to the probe electrical components.

The six insulated electrical wires exit the probe through an offset hole, 38.1 mm (1½-in) in diameter, in the nylon bearing plate and the abutting steel coupling bearing plate, 12.7 mm (½ in) thick.

The probe wires pass through the two bearing plates to make connection with underwater connectors on the electrical cables inside the Vibracore pipe. The steel bearing plate is welded into the coupler and is designed to absorb all vertical forces imposed on it by the resistivity probe. The coupler screws onto the Vibracore pipe by a 101.6-mm (4-in) IPS pipe thread.

Two small hand-held resistivity probes were developed to measure the conductivity of lithified core samples. However, no carbonate rock was encountered, so the instruments were not used.

3.3.2 Electronics

Equipment was chosen on the basis of reliability, delivery time, and ease of interfacing with NOAA's in-house development aids.

Critical components of the electronics system were calibrated by the manufacturer's laboratory following documented procedures and using equipment traceable to the National Bureau of Standards, within the limits of the Bureau's calibration services.

The resistivity probe system electronics are composed of three basic subsystems: signal generation, processing, and temperature monitoring (fig. 7).

Laboratory tests were conducted to determine an optimal range of frequencies for the source signal. At high or intermediate frequencies a capacitative component of the response interferes, and at very low frequencies polarization resistance interferes; the measurement instrumentation is

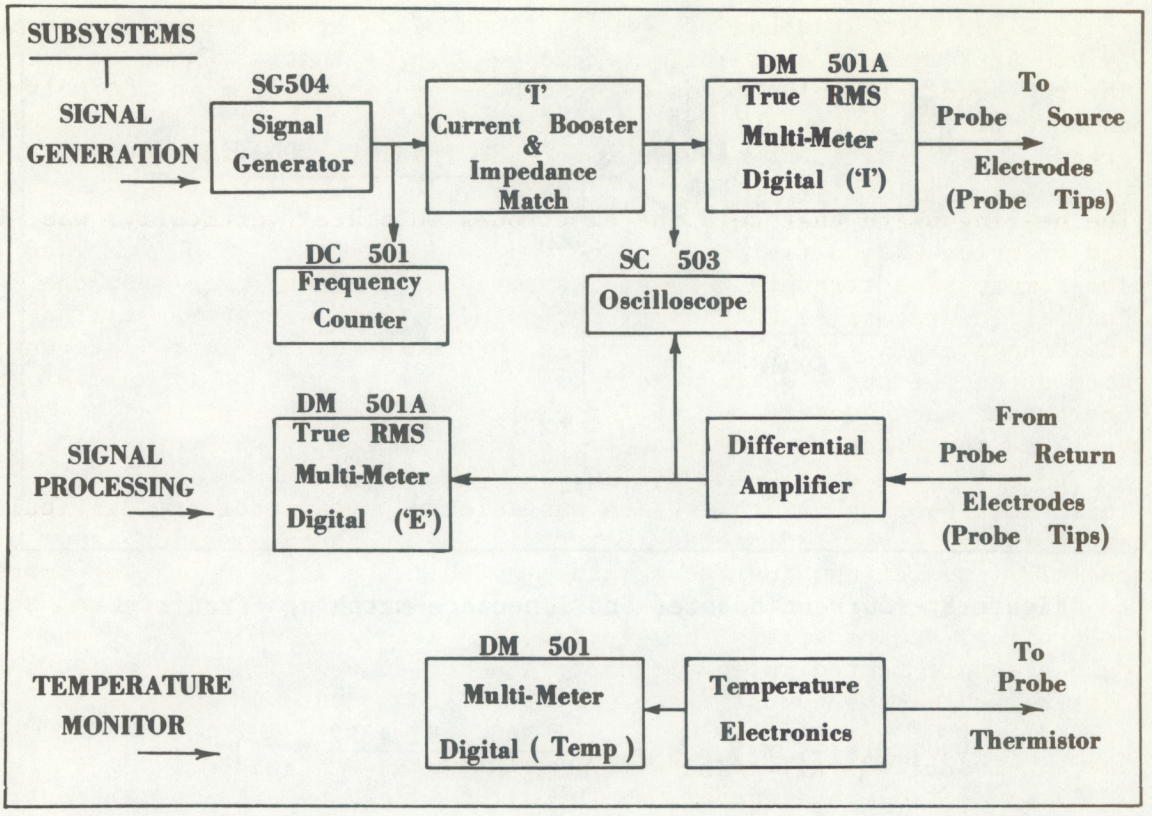

Figure 7.--Electronics system of resistivity probe.

not certified by the manufacturer. No interference was noted in the range 40 to 115 Hz; in the vicinity of 500 Hz the capacitative component was noted to have an effect less than 5 percent as large as the signal in material of the conductivity range of interest.

A Tektronix SG504 generator was used to provide a stable 100-Hz signal. The frequency was chosen to minimize noise problems caused by 60-cycle power-line disturbances and to minimize the polarization resistance components of the measurements.

Since extremely low resistances were expected, a current booster (fig. 8) and impedance-matching system were developed in-house, designed to keep loading of the output of the signal generator (SG504) from introducing distortion. The current booster and impedance-matching circuits were required to withstand long periods of nearly complete electrical short, yet have a very fast response time as the probe encountered higher resistances.

The signal from the current booster was monitored by a Tektronix true-RMS-reading DM501A digital multimeter prior to being sent to the source electrodes (fig. 7). The true-RMS-measuring capabilities of the meter eliminated some of the computer processing time for data reduction.

For the signal-processing electronics a high-impedance input "coarctation" amplifier (fig. 9) was developed to process the signal from the probe return electrodes. The mathematical equation for the coarctation amplifier is

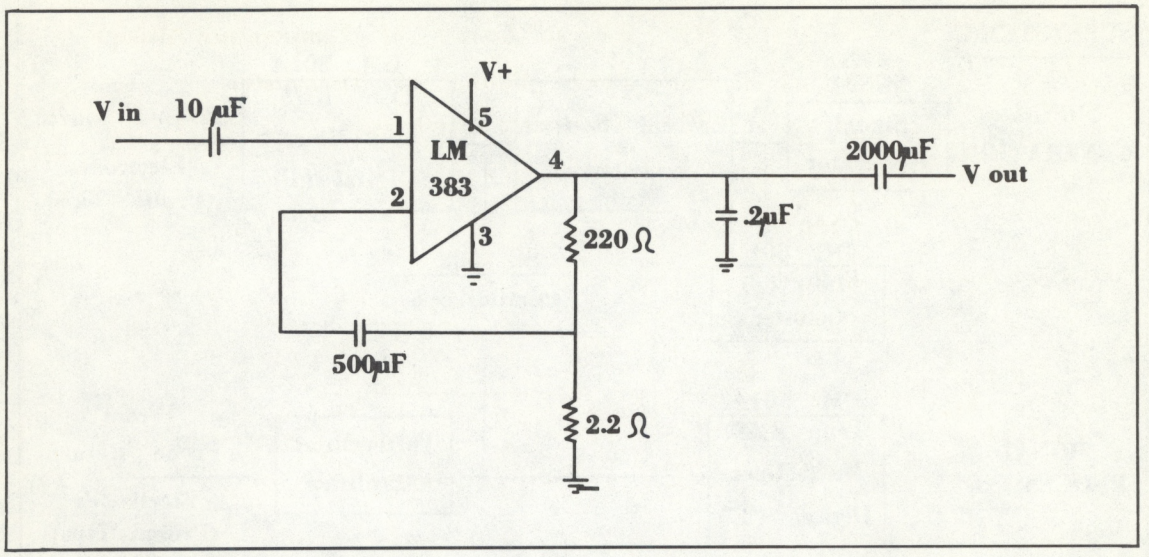

Figure 8.--Current booster and impedance-matching circuitry.

$$V_{out} = -\left(\frac{R2}{R1} \times V_{in1}\right) + \left[\left(\frac{R4}{R3 + R4}\right)\left(\frac{R1 + R2}{R1}\right)V_{in2}\right] .$$

The signal out of the coarctation amplifier is monitored by the true-RMS-reading multimeter (fig. 7).

A temperature-measuring system was used to monitor effects of heat caused by vibration of the probe tip as it encountered the stiff bottom material (fig. 10). The output voltage was monitored by a Tektronix DM501 DC voltmeter (fig. 7).

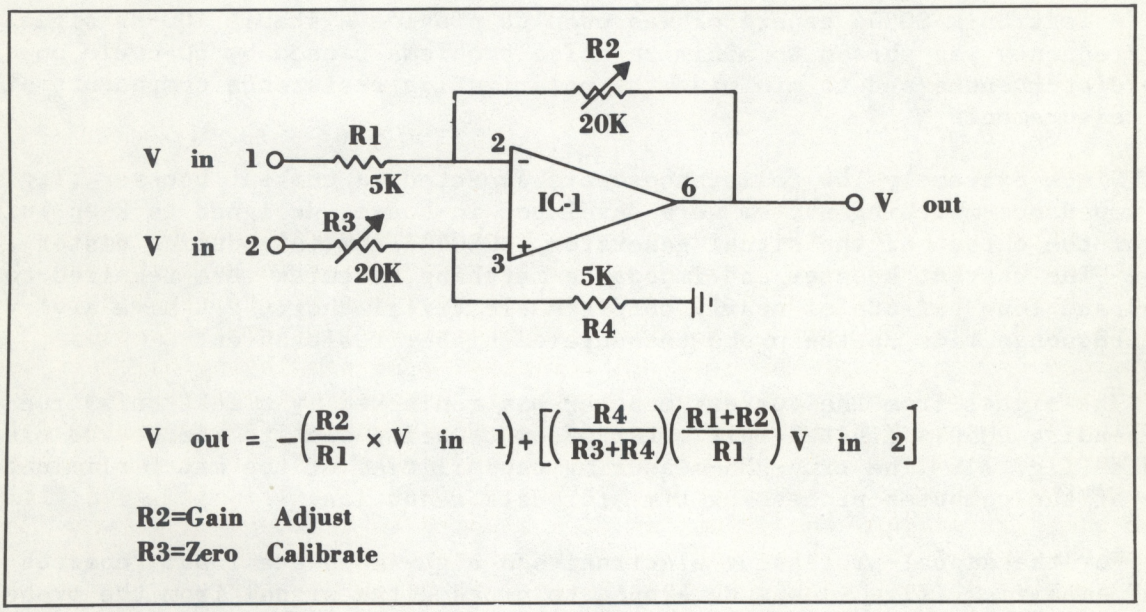

Figure 9.--Coarctation amplifier circuitry.

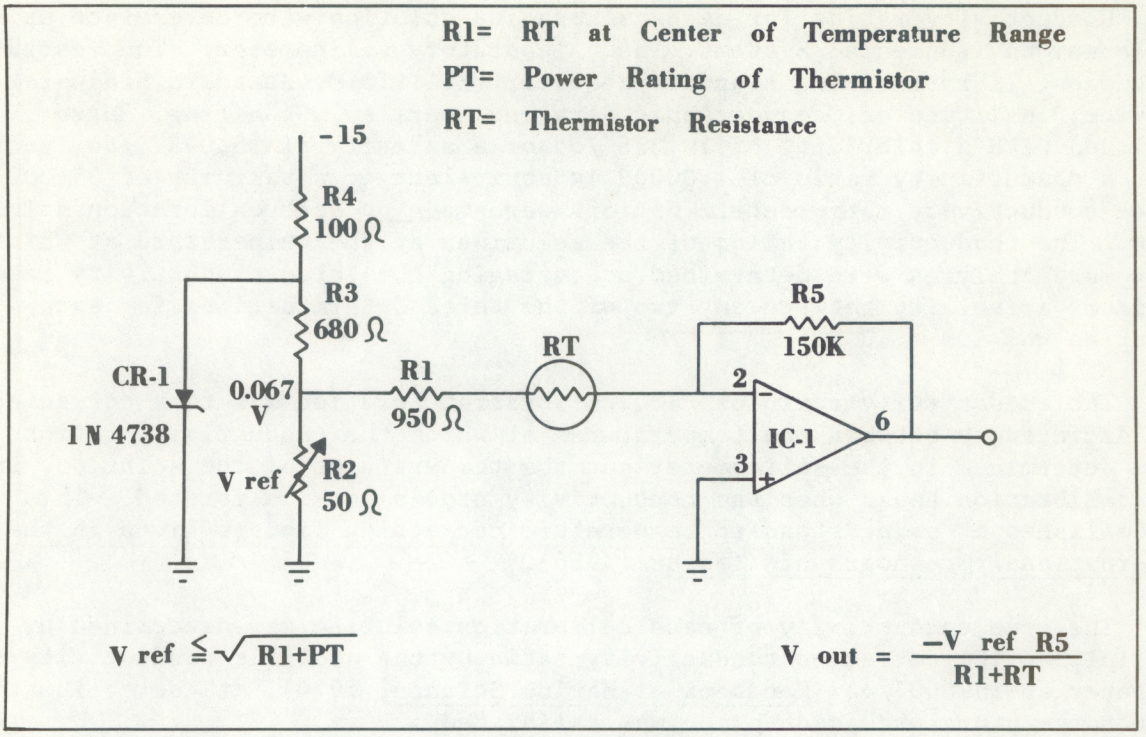

Figure 10.--Temperature monitor circuitry.

A Tektronix DC501 frequency counter and BC503 oscilloscope were used to monitor the output frequency and return signals during initial development of the system. They were not used during in situ measuring or calibration in order to minimize loading effects or introduction of errors into the measuring system.

4. CALIBRATIONS

4.1 Resistivity Probe

Calibration of the resistivity probe tips was accomplished by making admixtures of seawater and fresh water of varying ratios in polyethylene tanks (approximately 1.2 m [4 ft] in diameter by 1.5 m [5 ft] high), containing ~1.51 m^3 (400 gal) of solution. Appropriate tank dimensions were determined by monitoring the apparent resistivity as insulating barriers were placed in various geometries about a probe, in homogeneous electrolyte solutions. The tank dimensions used and the positions of probes within the tank were well removed from those that had noticeable effects on the apparent resistivity. Ratios of seawater to freshwater were 1:0, 1:1, 1:3, and 1:8. After thorough mixing, the solutions were allowed to stand overnight to assure consistent salinities and temperatures throughout each tank. Two-liter samples of each tank were then taken 1 ft below the surface (equivalent to the depth of the exposed electrodes below the water surface) for the determination of conductivity in each of the four calibration solutions.

Conductivity ratios for each calibration solution were determined using a Plessey Environmental Systems, Inc., laboratory salinometer. The instrument was calibrated using standard seawater (I.A.P.S.O. Standard Sea-Water Service, Institute of Oceanographic Services, Wormley, Godalming, Surrey, England) with a chlorinity of 19.376°/oo or a salinity of 35.0037°/oo, such that a conductivity ratio of 1.00000 is equivalent to a salinity of 35.000°/oo. Three conductivity ratio determinations were made on each calibration solution. The conductivity ratios of the solutions at the temperature at which they were analyzed were determined by averaging the three conductivity ratios. Maximum variability between any two of the three determinations for each solution was 1.0×10^{-4}.

The conductivity ratio of each calibration solution was then corrected for differences between the temperatures at which the conductivity ratios were determined in the salinometer and the temperatures of the solutions in the calibration tanks when the conductivity probes were calibrated. This was accomplished by using standard temperature correction factors given in the International Oceanographic Tables (1966).

The true conductivity of each calibration solution was determined by multiplying the corrected conductivity ratio by the specific conductivity of seawater at 35.000°/oo (Handbook of Marine Science, 1974), at the calibration tank temperature when each probe was calibrated.

Each conductivity probe was calibrated by immersion (electrode tips approximately 0.3 m [12 in] below tank water surface) in each of four calibration solutions during pre-field-study tests (conductivity ratios of solutions: 0.97756, 0.52581, 0.28239, and 0.14961 based on a conductivity ratio of 1.00000 for standard seawater with a salinity of 35.000°/oo) and in three calibration solutions during post-field-study tests (conductivity ratios of solutions: 0.98670, 0.28687 and 0.13181 based on 1.00000 for standard 35.000°/oo seawater).

Between measurements in each solution, the probe and electrodes were wiped dry to eliminate contamination from one tank to the next. Each calibration tank was grounded by using a piece of copper screen 0.2 m (8 in) × 0.46 m (18 in), grounded through a cable to the electronics system. All cables and electronic equipment were the same as those used during field testing.

In each calibration solution approximately 0.6 V (measured at the output terminals without the probe attached) at 100 Hz alternating current was applied to each probe while six measurements of resistance were recorded at 30-s intervals. The maximum variability in the resistance readings occurred in the high-conductivity solutions and was on the order of ±0.002 ohm.

The six values of resistance were averaged for each probe in each calibration solution. The reciprocals of these averages were plotted against the true conductivity value of each calibration solution. Best-fit least-squares lines were determined by computer for each probe in both pre- and post-field-study calibrations (figs. 11-16). All correlation coefficients were better than 0.999. Example calculations can be found in Appendix A.

The vertical extent and the volume of material making the primary contribution to conductivity probe response were determined in the tanks of solutions

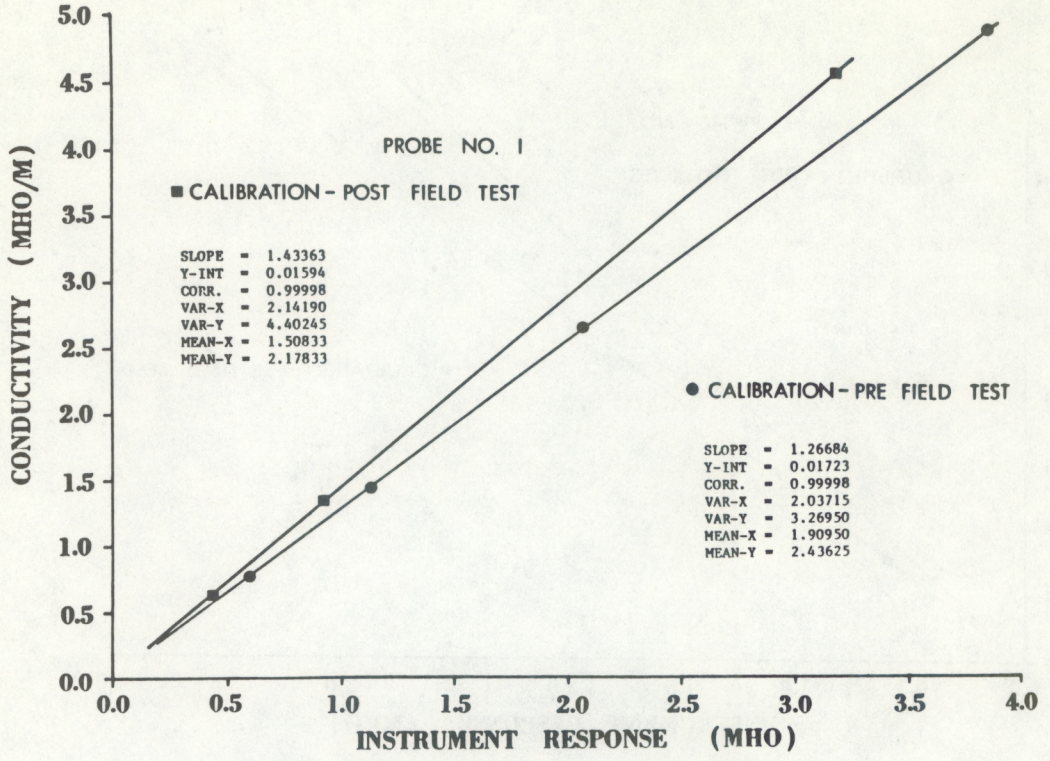

Figure 11.--Calibration data: pre- and post-field-study tests, probe 1.

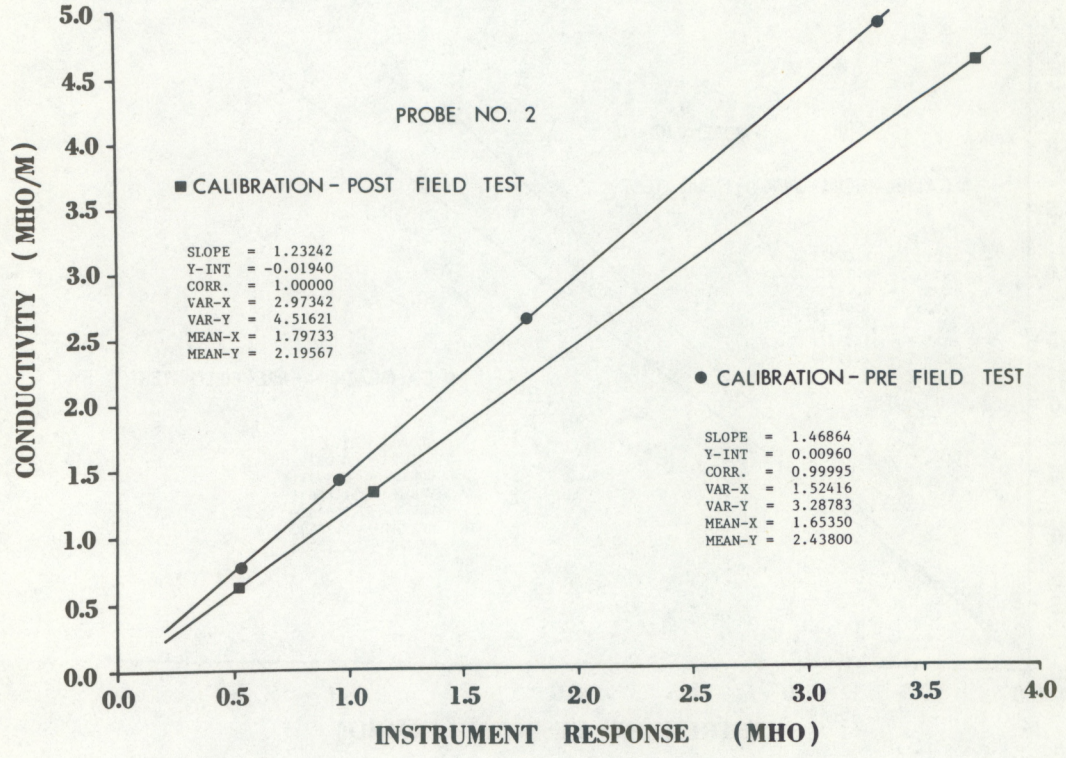

Figure 12.--Calibration data: pre-and post-field-study tests, probe 2.

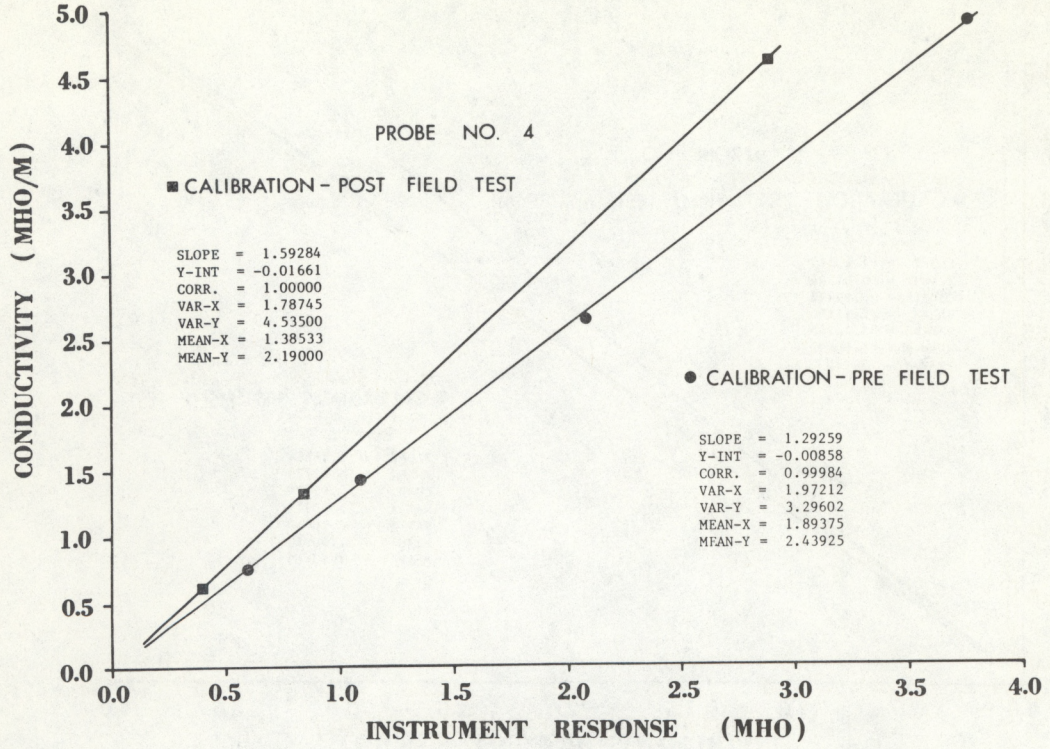

Figure 13.--Calibration data: pre- and post-field-study tests, probe 3.

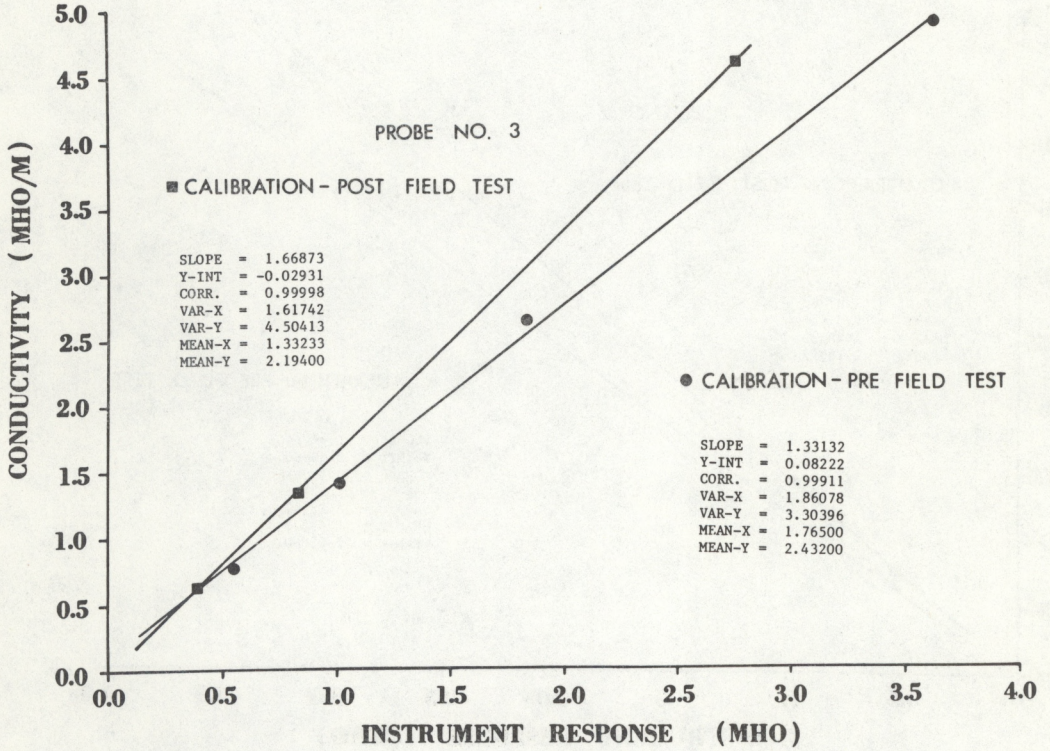

Figure 14.--Calibration data: pre- and post-field-study tests, probe 4.

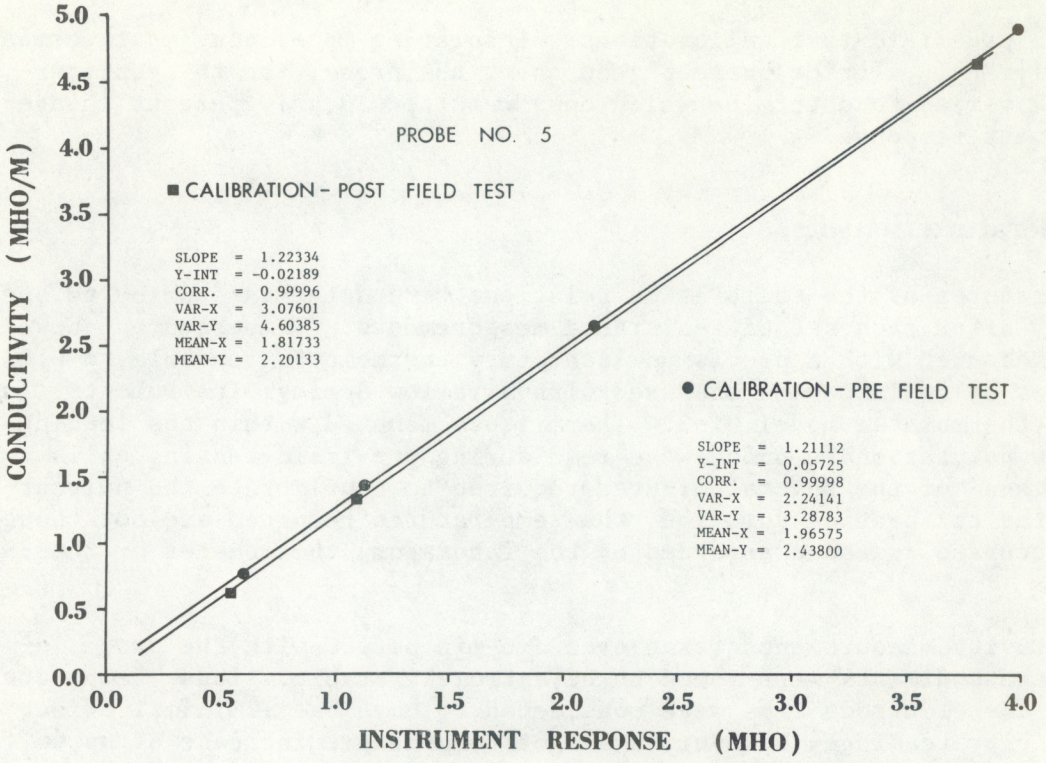

Figure 15.--Calibration data: pre- and post-field-study tests, probe 5.

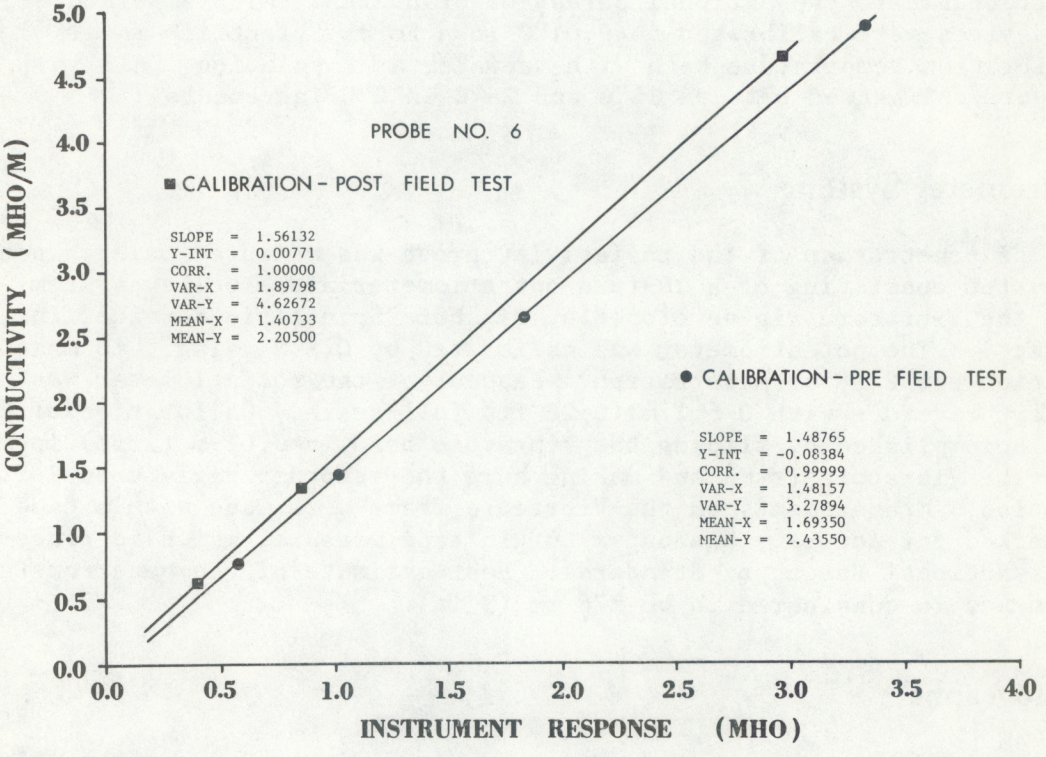

Figure 16.--Calibration data: pre- and post-field-study tests, probe 6.

used in the pre-field-test calibrations. Insulating materials (most commonly made of polyvinyl chloride) were placed about the probe, and the configurations were varied to determine which ones resulted in a 10 percent change in the instrument response.

4.2 Temperature Sensors

Temperatures of the calibration solutions were determined prior to and immediately after each set of resistance measurements. Temperatures above 19°C were measured with a precision laboratory thermometer readable to 0.01°C. Temperatures below 19°C were measured with a Yellow Springs Instruments, Inc., electronic thermometer model OT-2. Thermistors mounted within the leading edge of the polycarbonate probe were read during pre-field-testing calibrations. Because of the several minutes required to equilibrate the polycarbonate to the calibration solution, the temperatures recorded are not thought to be as accurate as those recorded by the laboratory thermometer or the YSI probe.

Resistivity measurements taken over a 6-min period with the probe inserted in the sediments were found to be extremely stable. Thus, temperature changes at the electrode tips were considered to have had a minimal effect on the resistivity readings; however, a slight temperature increase of up to 0.75°C was considered when the estimated limits of uncertainty of the reported data were established.

Prior to field testing, the thermometers, YSI probes, and resistivity probe thermistors were calibrated against a Hewlett-Packard model 2801A quartz thermometer, which has been calibrated by the manufacturer against standards traceable to the National Bureau of Standards. All temperature-measuring devices were calibrated to 0.01°C in a Forma Scientific model 16-120 calibration temperature bath with tapwater as a solution. All instruments were calibrated between 15°C and 25°C in 2°C increments.

4.3 Penetrometer System

Depth of penetration of the resistivity probe was measured using a penetrometer system consisting of a 10-turn potentiometer and a pulley system mounted on the Vibracore rig developed by Offshore Scientific Service, Inc. (O.S.S., Inc.). The potentiometer was calibrated by O.S.S., Inc., to make one revolution per 2 ft of penetration. Readout of the potentiometer was on a strip chart recorder with 0-6.1 m (0-20 ft) full-scale. Calibration of the system was accomplished by sliding the Vibracore head in 0.61-m (2 ft) increments down the Vibracore frame and making sure the recorder registered 2 ft of penetration. Measurements on the Vibracore frame were made with a tape measure checked for accuracy against a Lufkin tape measure, which is traceable to the National Bureau of Standards. Best estimate of the penetrometer system accuracy is considered to be ±76 mm (3 in).

4.4 Chronographs

All values of time were recorded from quartz digital chronographs calibrated against radio station WWV of the National Bureau of Standards. No detectable variation from the standard was noted.

5. FIELD ACTIVITIES

5.1 Seismic Survey

A detailed seismic survey of the study area was completed using an EG&G Uniboom shallow-penetration seismic-reflection profiling system. Navigation was accomplished with shore-based twin theodolite towers. The survey covered 9.2 km of trackline. Seventeen lines approximately 316 m long and 61 m apart were run north-south over an east-west rectangle 975 m long. Three east-west lines crossed the north-south lines and extended 305 m farther east. Figure 4 shows the location of the seismic tracklines and the resistivity probe sites.

The seismic survey delineated the sedimentary structures in the series of linear ridges and plateaus aligned north-south as described above. The low at the study site, between the second and third reef, is nearly acoustically transparent except for a strong reflector 0.3 m thick lying 2 to 2.5 m beneath the sediment surface (figs. 17 and 18). This layer consists of larger coral and mollusk fragments packed together with sand forming a very dense layer and a good acoustic reflector. This reflector can be traced through the second and third reefs and across the second plateau (fig. 17).

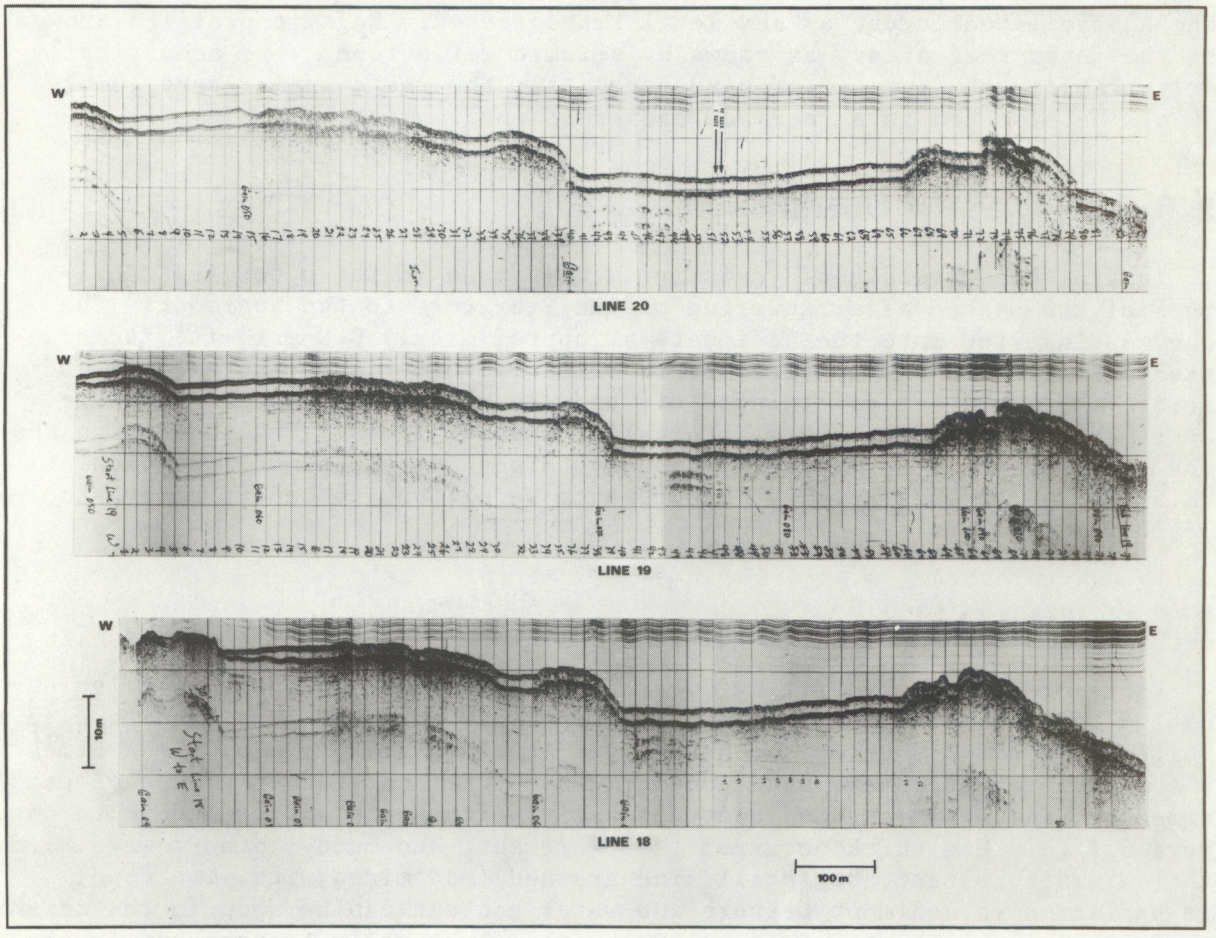

Figure 17.--Seismic records from east-west trending tracklines.

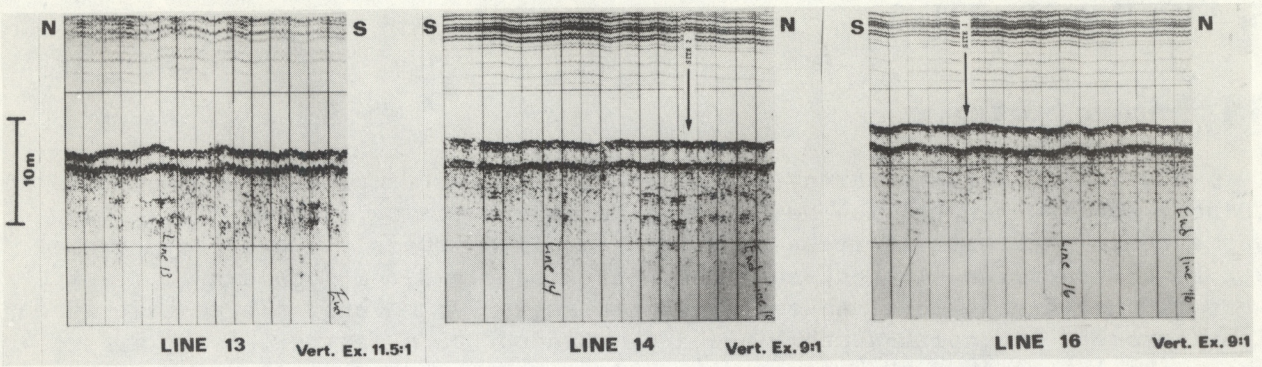

Figure 18.--Seismic records from north-south trending tracklines across the resistivity probe sites.

Depth to the reflector varies only slightly over the whole study area, even over the reefs. It is suggested that this layer may be an unconformity marking the death of the outer barrier reef organisms. Subsequent deposition of large amounts of coral rubble occurred in the depression behind the reef. During this time the second reef began growing coral on the old coastal dune ridge and soilstone crust as sea level transgressed. Seismic profiles showed that the inter-reef areas, as shown by seismic reflection, were acoustically nearly transparent (typical of sand deposits); the reefs appear very jumbled as would be expected in a reef and back-reef environment.

5.2 Resistivity Probe Operation

Initial measurements of resistivity were made in the upper few centimeters of the seabed after lowering of the Vibracore to the seafloor. The probe was inserted into the sediments at approximately 0.3-m (1-ft) increments to the limit of the Vibracore or refusal. After each incremental insertion, the Vibracore was turnned off and six resistivity and temperature measurements were made at 30-s intervals for about 3 min. The current to the probe electrodes was applied continuously throughout the probe insertion at each site, and the resistivity measurements were found to be extremely stable at each increment.

5.3 Coring and Drilling

Vibracore and rock-drilling operations in the third plateau revealed unconsolidated sediment down to subbottom depths of at least 10 m, and to 11.3 m at site 2B (fig. 4). Below the hard layer at approximately 2 m, the sediment was a mixture of carbonate sand and mud with occasional larger pieces of coral fragments. The water and mud contents varied with depth and from core to core. Layers 0.1 to 0.2 m thick occurred that were soft and muddy; others were hard, with low water content, but still fine-grained (mud mixed with some sand). This variation in sediment texture and water content can be seen in the seismic records as faint reflectors alternating with acoustically transparent layers. Figure 19 shows typical sediments found in the topographic low between the second and third reefs.

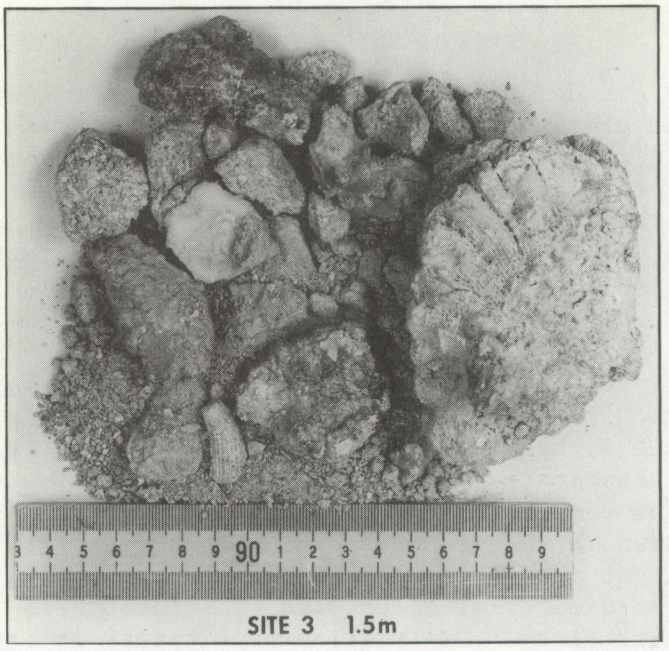

Figure 19.--Photograph of typical carbonate sediment near the array.

Table 1 shows the drilling statistics for coring operations at sites 2A, 2B, and 6. The last column shows the total number of blows (48.4 kg-m, 350 ft-lb each) required to drive the bottom 0.3 m (1 ft) of the 0.6-m (2-ft) core barrel. Data for the upper 0.3 m were discarded because the material was always loose sand that remained after washing out the casing.

Table 1.--Drilling statistics

Site	Hole no.	Depth (m)	Total blows in bottom 0.3 m
2A	1	2.7-3.0	32
2A	1	4.3-4.6	12
2A	1	5.5-5.8	265
2B	2	3.4-3.7	32
2B	2	6.4-6.7	23
2B	2	7.9-8.2	6
2B	2	9.4-9.7	12
2B	2	11.0-11.3	20
6	3	3.4-3.7	81
6	3	4.9-5.2	71
6	3	6.4-6.7	64
6	3	7.9-8.2	142
6	3	9.4-9.7	71

6. RESULTS

Conductivity measurements were made at six sites, five within the third plateau area and one in the second plateau (fig. 4). Uniboom seismic data were reinterpreted following field coring of sediments. Table 2 summarizes the seismic stratigraphy at each penetration site. Hard and soft sedimentary layers have been delineated from the profiles (figs. 17 and 18). These seismic data were correlated visually with conductivity and rate-of-penetration data. Seismic records from each field site were abstracted from the full suite of records.

Conductivity data plotted for each site are depicted in figs. 20-25. (Instrument response and uncorrected resistivity/conductivity field data are given in Appendix B.) Bars in each figure represent the limits of uncertainty in the conductivity data. Best estimates of the actual conductivity are indicated by a box at each level of penetration. The uncertainty in the data arises from two sources: (1) changes in the geometry of the measured portion of the electrical field due to slight mechanical changes in the conductivity probe during penetration through hard material (electrical insulation was deformed), and (2) calibration uncertainty. Calibration uncertainty is estimated at less than 0.5 percent of the measured calibration values. The primary contribution to the limits of uncertainty varied from ±2 percent to ±15 percent. Changes in electrode geometry due to deformation of the insulation about the probe tips can increase or decrease the response factor of the probe; for example, exposure of a portion of the outer electrodes that is nearest the inner electrode tips would result in a change such as that seen with probe 1 (fig. 11); the opposite change would occur with partial exposure of the far sides of the outer electrodes (fig. 12). Our best estimates of the conductivity (table 3) represented by the boxed data (figs. 20-25) are based on the assumptions of the next paragraph and are considered to be representative to within ±3 percent of the estimated values. The estimated values at each data point (depth of penetration) were determined by analysis of rate of penetration and probe calibration data (calibrations carried out before and after field tests, figs. 11-16).

Negligible deformation of the probe insulation is expected to have occurred during the initial sediment penetration of the conductivity probes. Deformation began upon contact with hard sedimentary layers as indicated by the plots of penetration rate versus depth (figs. 26-31). Deformation is believed to have occurred progressively as additional hard layers were encountered, with the greatest deformation occurring in the hardest layers. Thus, the appropriate calibration for the initial data point would be that made before the field test; the calibration for the deepest data point would be that made after the probe was used in the field. The indicated range of uncertainty in other values measured for conductivity includes the conductivities calculated using both the predeployment calibration and the postdeployment calibration. To assess the maximum effect insulation deformation might have on the conductivity readings, the electrodes of one probe were completely stripped of insulation after recalibration and the probe was tested again (fig. 32). Even gross changes in the geometry of the exposed electrodes gave only moderate changes in the calibration line, particularly in the range of conductivities of interest.

It should be noted that the final data points at all sites, except site 5, were obtained in material that the probe could not penetrate. At

Table 2.--Seismic stratigraphy

Site No.	Depth (m)[1]	Description
1	0-0.3	soft
	2	slightly hard reflector
	7.6-2.3	soft
	2.3-2.4	very hard reflector
	2.9-3.0	slightly hard reflector
	4.3-4.6	slightly hard reflector
	5.2-5.5	slightly hard reflector
	5.8	slightly hard (approx. 0.3 m thick) reflector
	7.3	slightly hard reflector
2, 2A, 3	0-0.46	soft
	0.46-0.76	slightly hard reflector
	0.9-2.0	soft
	2.0-2.3	very hard reflector
	2.4-2.7	slightly hard reflector
	4.6-4.9	slightly hard reflector
	7.3-7.6	slightly hard reflector
4	0-0.9	very hard reflector
	1.8-2.4	hard reflector
	Seismic data indicate entire section from 0 to 6.1 m is considerably harder than equivalent section at sites in "lows.")	
5	0.76-1.1	slightly hard reflector
	1.5-1.8	very hard reflector
	3.0-3.4	slightly hard reflector
	4.6-4.9	slightly hard reflector
	5.2-5.5	slightly hard reflector
	6.1-6.4	slightly hard reflector
	7.0-7.3	slightly hard reflector

[1]Depth uncertainty of approximately 0.3 m due to swell.

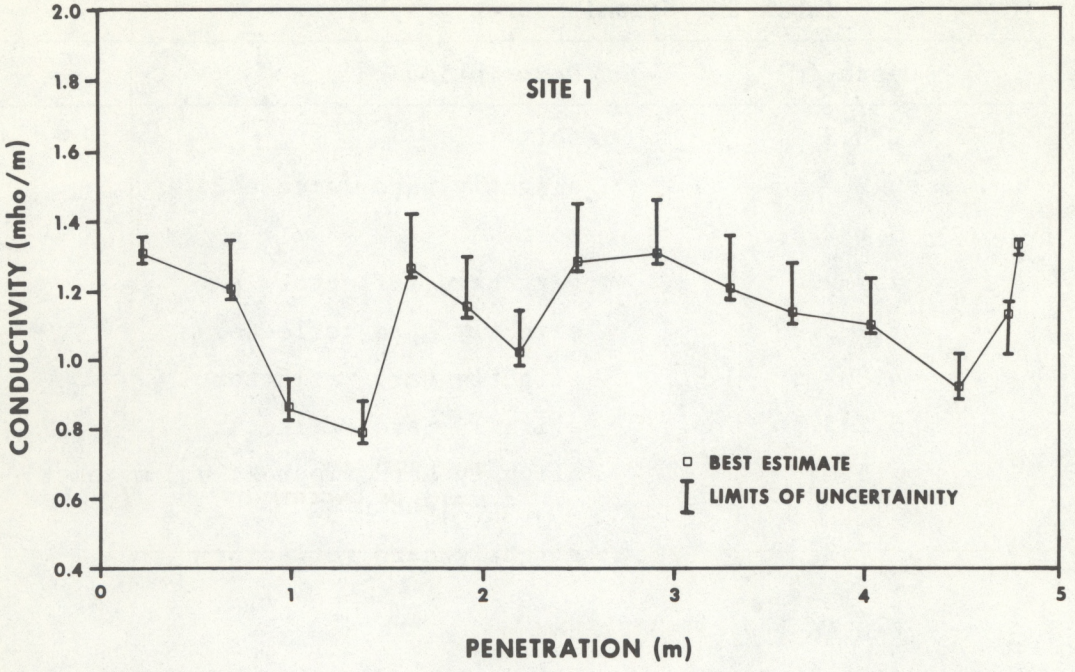

Figure 20.--Conductivity data vs. depth, site 1.

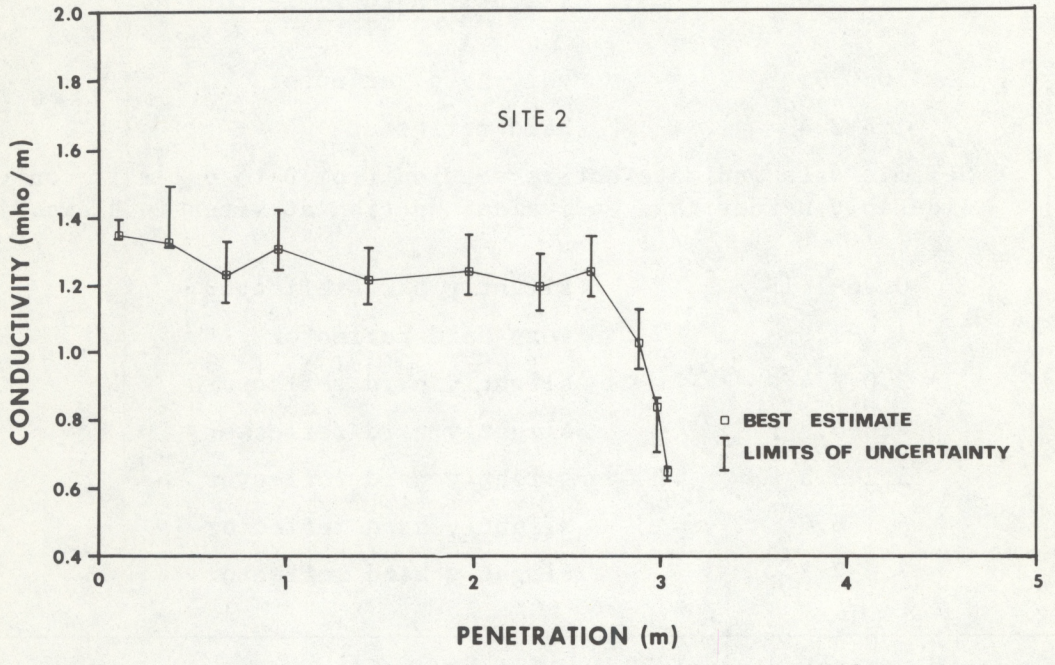

Figure 21.--Conductivity data vs. depth, site 2.

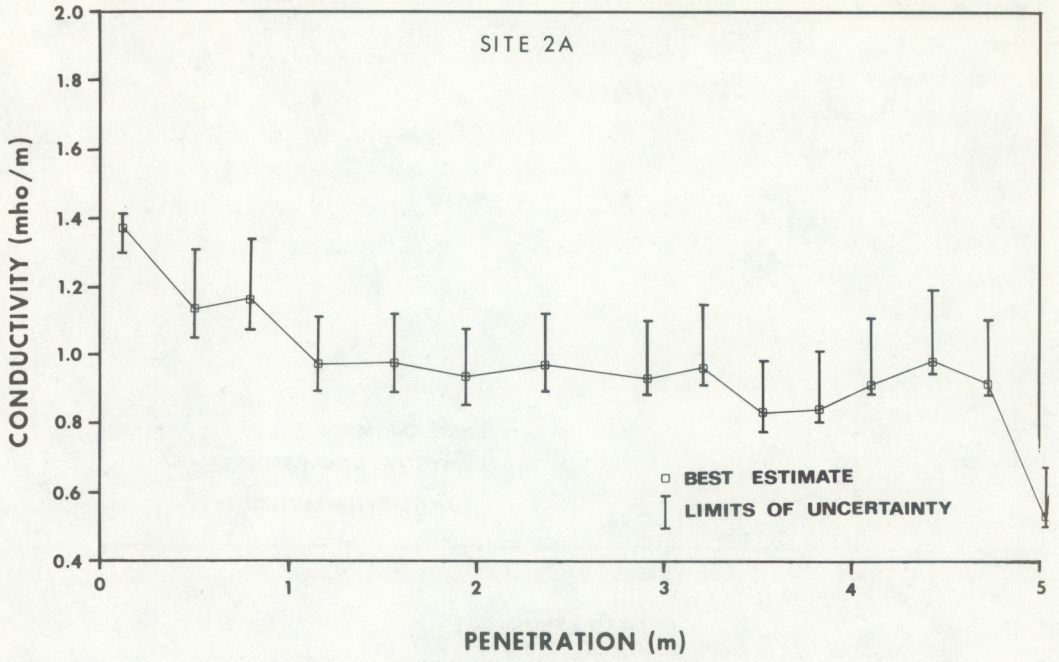

Figure 22.--Conductivity data vs. depth, site 2A.

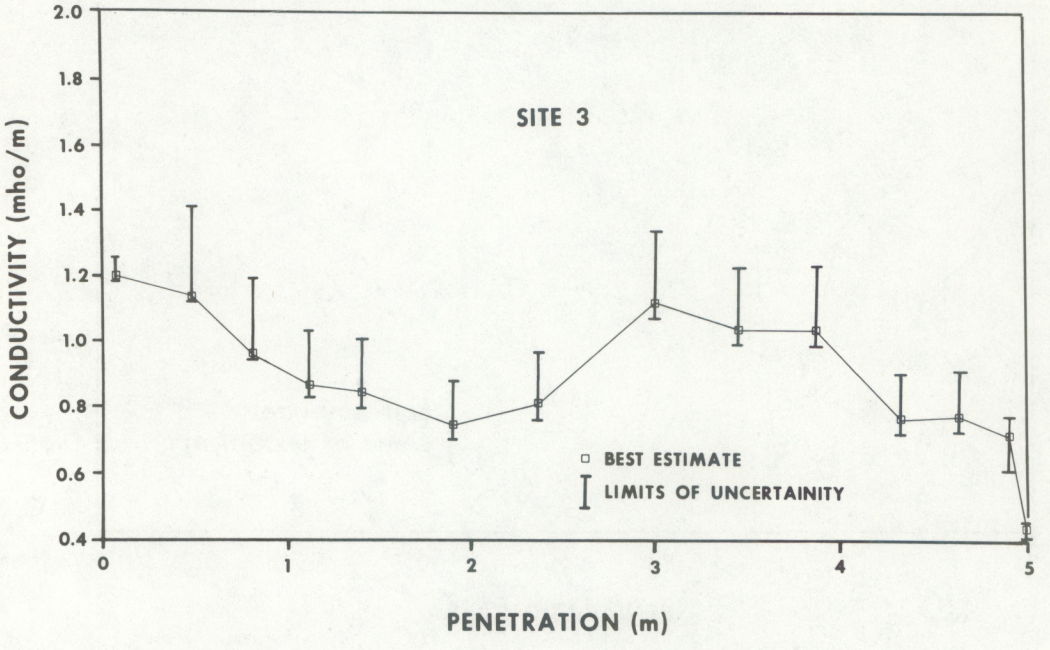

Figure 23.--Conductivity data vs. depth, site 3.

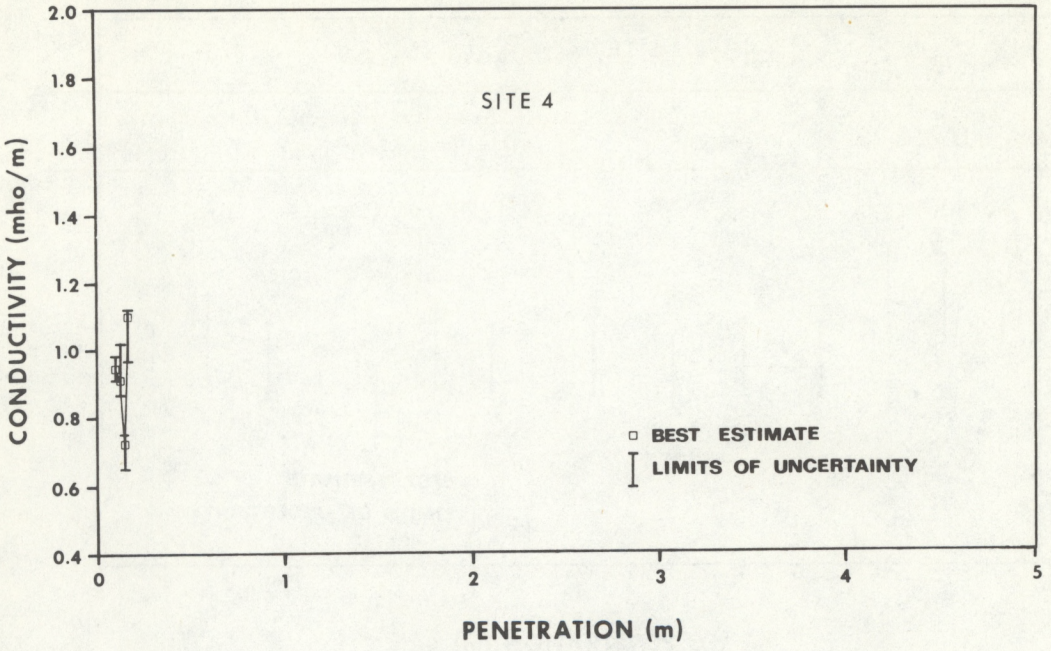

Figure 24.--Conductivity data vs. depth, site 4.

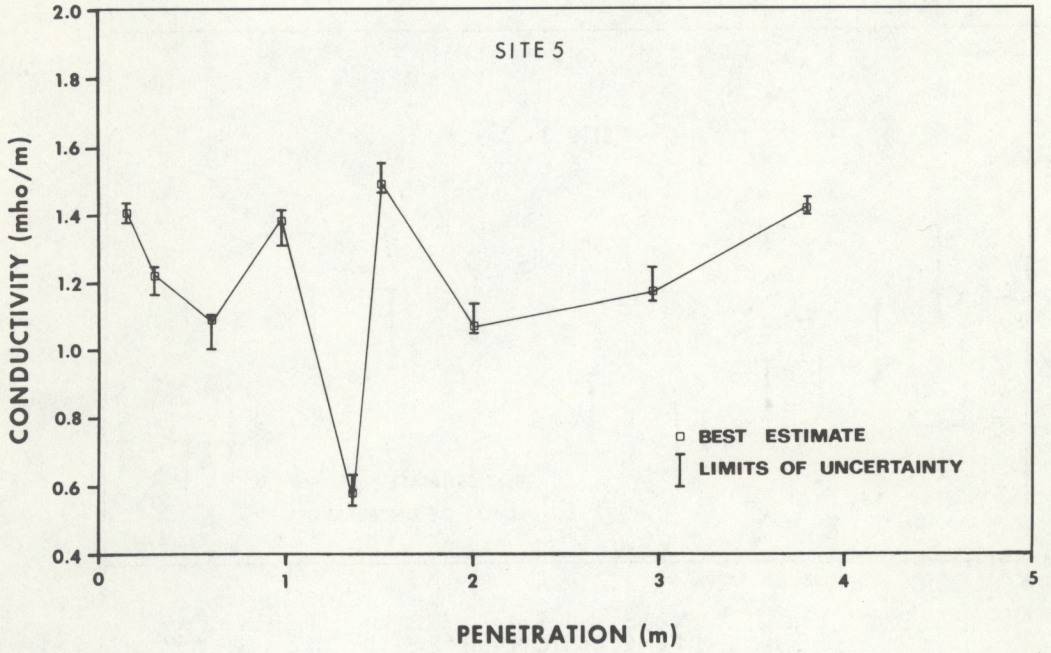

Figure 25.--Conductivity data vs. depth, site 5.

Table 3.--Best estimate of conductivity with depth at each probe site

Depth below sediment/ water interface (m)	Conductivity (mho/m)
SITE 1	
0.23	1.31
0.69	1.20
0.99	0.85
1.37	0.79
1.62	1.26
1.91	1.15
2.19	1.02
2.49	1.29
2.90	1.31
3.28	1.21
3.61	1.14
4.01	1.10
4.47	0.92
4.72	1.14
4.78	1.33
SITE 2	
0.10	1.35
0.38	1.33
0.68	1.23
0.97	1.32
1.45	1.22
1.98	1.25
2.36	1.20
2.64	1.25
2.90	1.04
3.00	0.84
3.02	0.65
SITE 2A	
0.10	1.38
0.48	1.14
0.79	1.17
1.14	0.98
1.55	0.98
1.93	0.94
2.36	0.97
2.90	0.94
3.20	0.97
SITE 2A (continued)	
3.50	0.83
3.81	0.84
4.09	0.91
4.42	0.99
4.70	0.92
5.03	0.52
5.08	0.81
SITE 3	
0.08	1.20
0.48	1.13
0.81	0.96
1.12	0.86
1.40	0.84
1.91	0.74
2.36	0.80
3.00	1.11
3.45	1.03
3.86	1.03
4.32	0.76
4.62	0.77
4.90	0.71
5.00	0.43
SITE 4	
0.10	0.95
0.13	0.91
0.15	0.72
0.16	1.10
SITE 5	
0.15	1.42
0.30	1.23
0.61	1.09
0.99	1.40
1.37	0.56
1.52	1.50
2.01	1.06
2.97	1.17
3.81	1.43

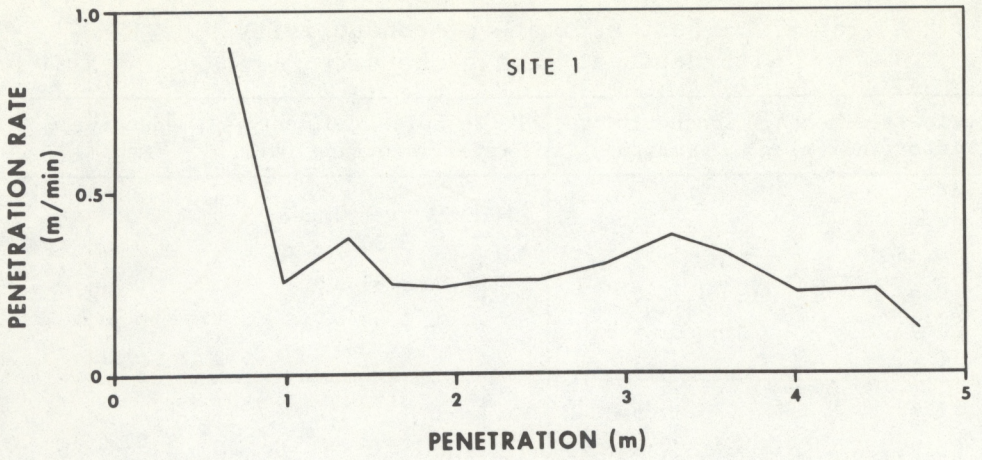

Figure 26.--Probe penetration rate vs. depth, site 1.

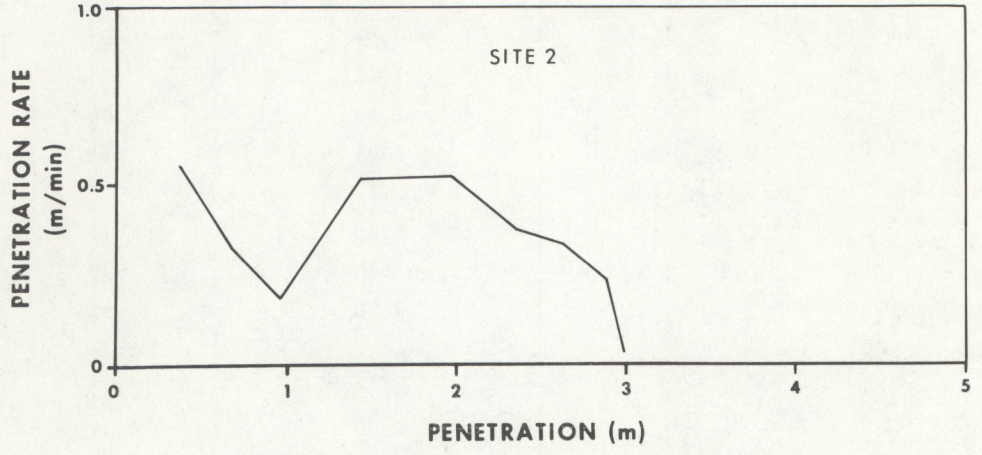

Figure 27.--Probe penetration rate vs. depth, site 2.

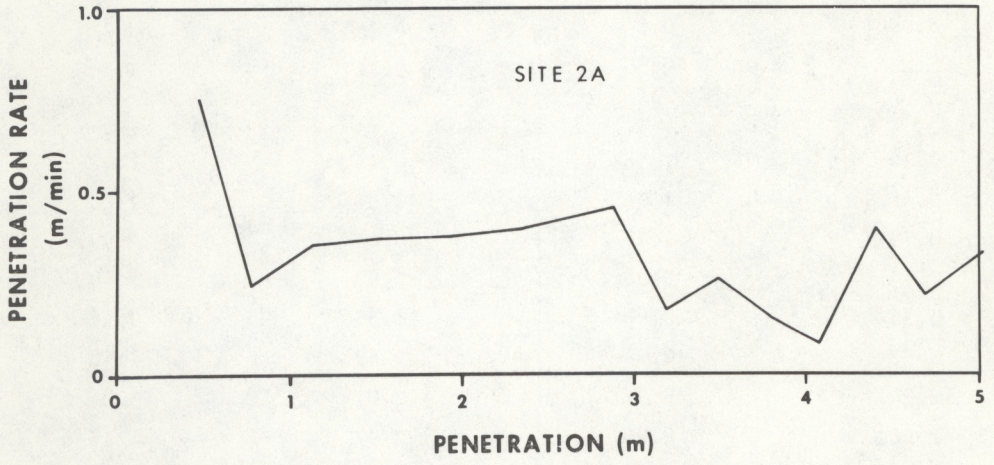

Figure 28.--Probe penetration rate vs. depth, site 2A.

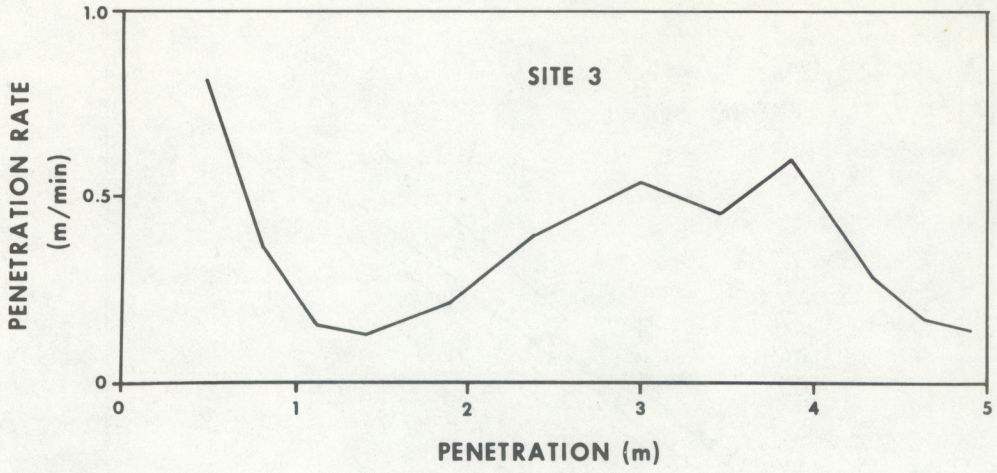

Figure 29.--Probe penetration rate vs. depth, site 3.

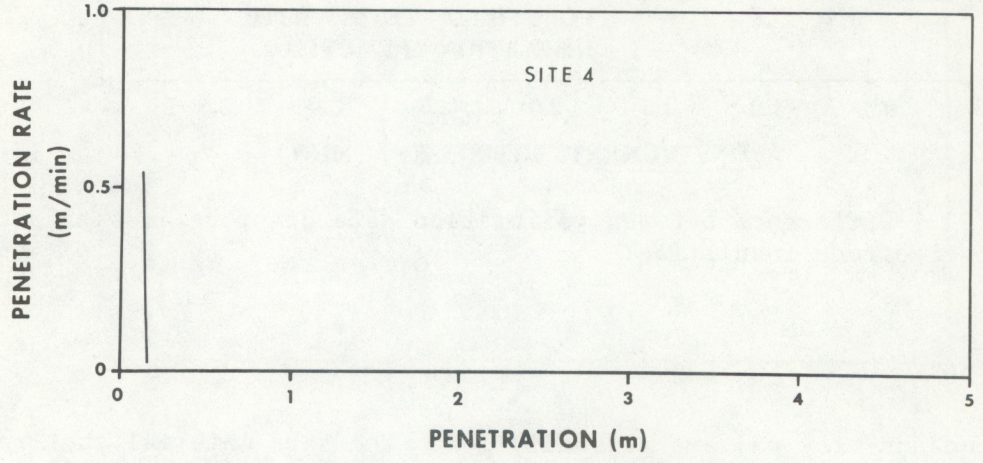

Figure 30.--Probe penetration rate vs. depth, site 4.

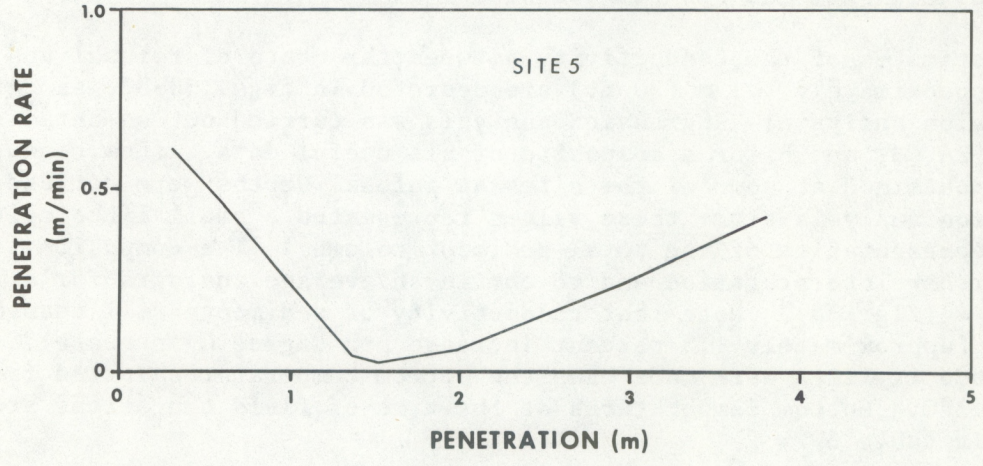

Figure 31.--Probe penetration rate vs. depth, site 5.

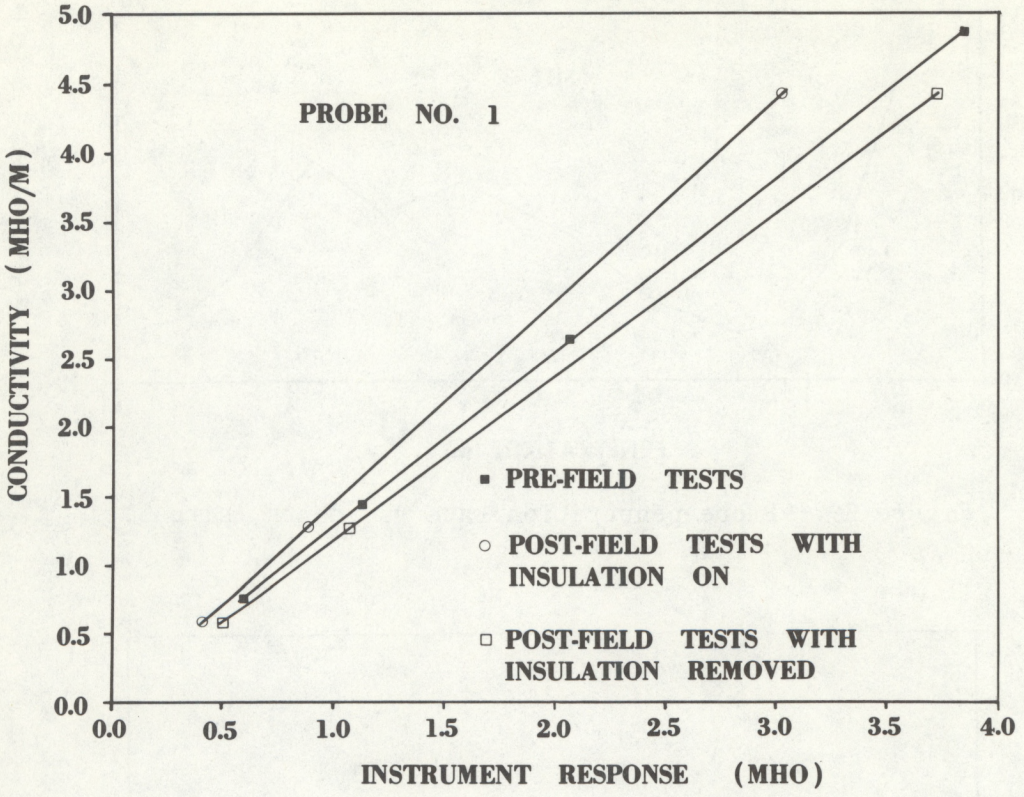

Figure 32.--Difference between calibration data of probe 1, with and without electrode insulation.

some sites conductivity was exceptionally low. The hard material that refused entry is presumed to be relatively thin sedimentary layers. We believe that below these hard layers the sediments become relatively softer and that the sediments have somewhat higher conductivities below the refusal depths (compare figs. 21-22). Tables 4 and 5 indicate which probes were used at each field site and the tests carried out at each site.

Best estimates of the conductivity between the depth of refusal and depths of approximately 9.1 m (30 ft) are depicted in figs. 33-37, as derived from regression analysis. Regression analysis was carried out on data from sites 1, 2, 2A, 3, and 5 for a composite of all useful data. (Low conductivity values obtained at some of the sites at refusal depths were not used in the regression analysis since these values represented a small lithologic unit not representative of the total sediment column.) The composite was used for further interpretation and to obtain an average analysis for all sites except site 4 (fig. 38). Note that conductivity of sediments will change with temperature (approximately 1.5 percent increase per degree C increase). The reported conductivities were made when the bottom temperatures varied from 21.7° to 22.3°C. Bottom temperatures at the time of field operations are summarized in table 6.

Table 4.--Probes used at study sites

Site No.	Probe No.
1	1
2	6
2A	2
3	4
4	3
5	5

Table 5.--Field operations at study sites

Vibracore	1, 2, 2A, 3, 4, 5
Probe	1, 2, 2A, 3, 4, 5
Drill core	2A, 2B, 6

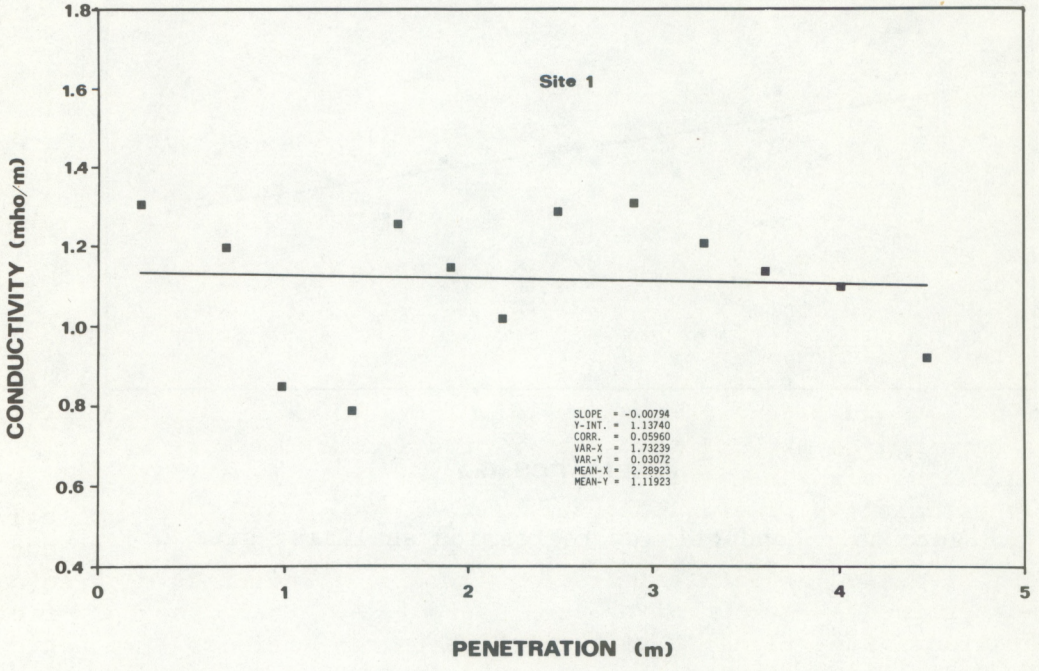

Figure 33.--Conductivity regression analysis, site 1.

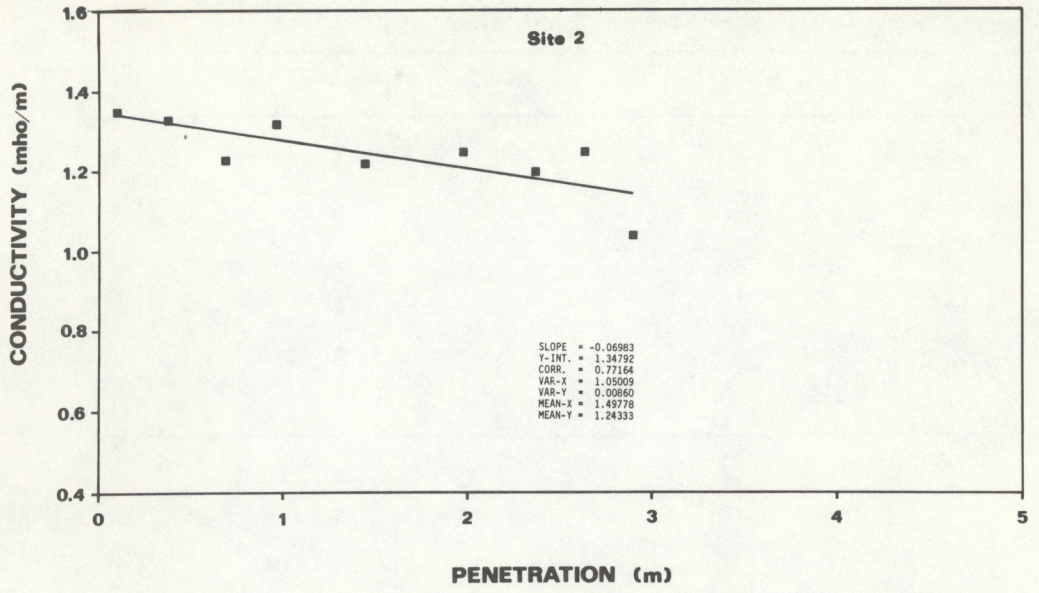

Figure 34.--Conductivity regression analysis, site 2.

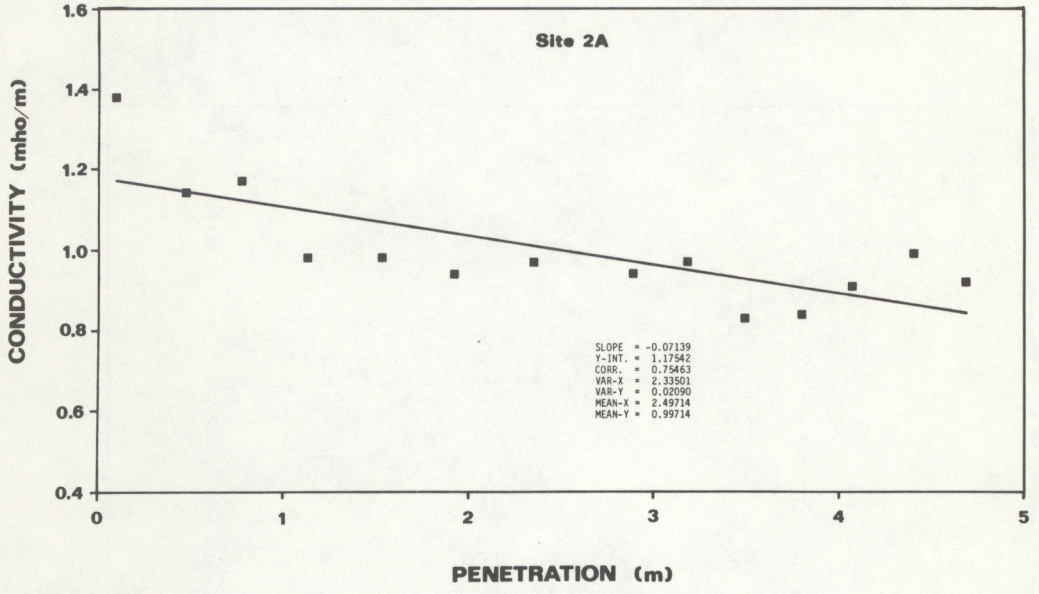

Figure 35.--Conductivity regression analysis, site 2A.

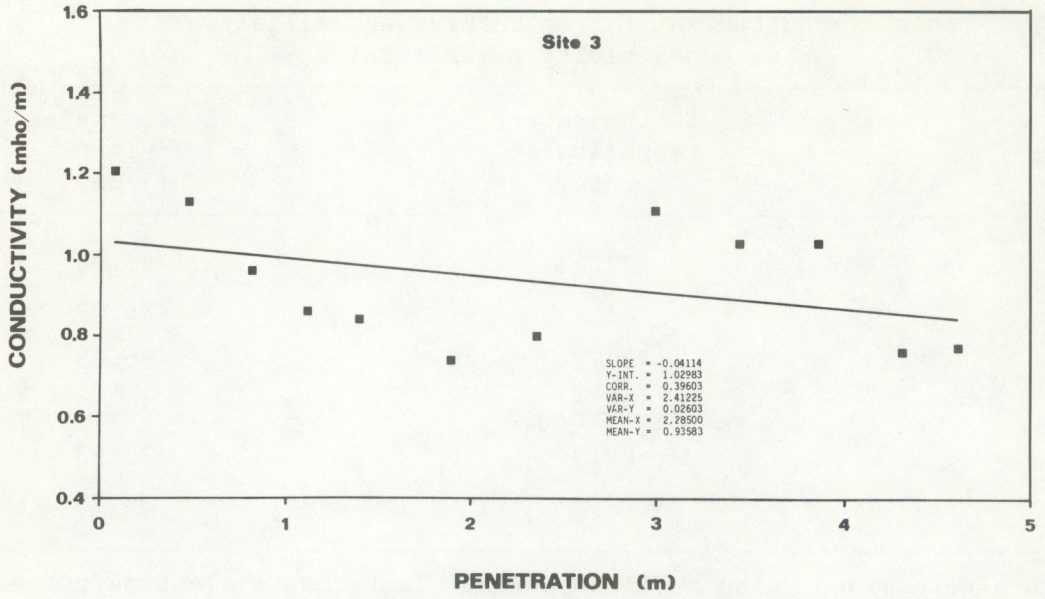

Figure 36.--Conductivity regression analysis, site 3.

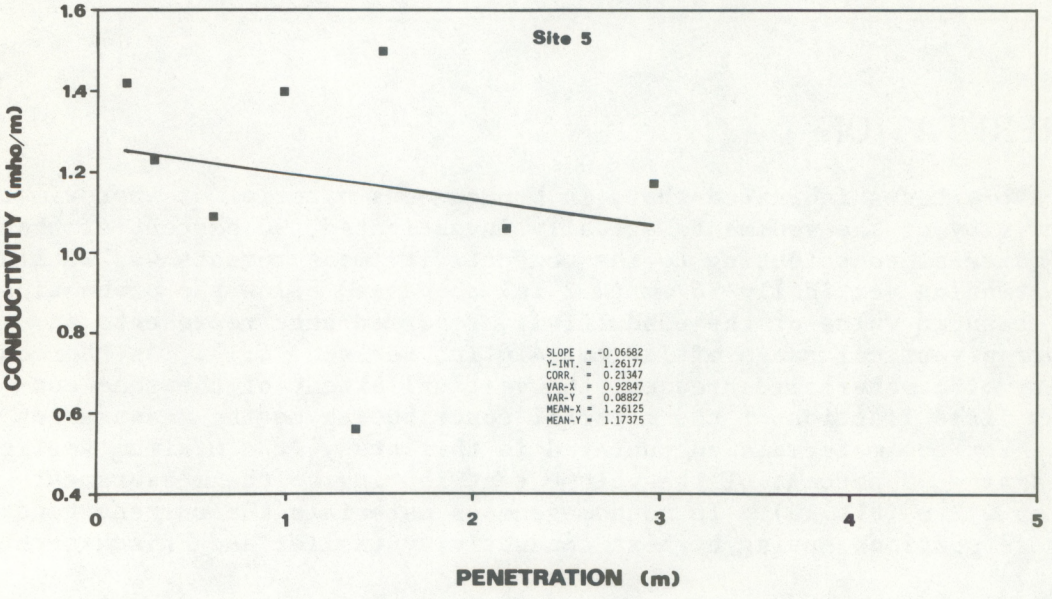

Figure 37.--Conductivity regression analysis, site 5.

Table 6.--Bottom water temperatures and salinities at conductivity probe sites

Site no.	Bottom-water temperature* (°C)	Bottom-water salinity** (°/oo)
1	22.2	36.06
2	21.7	36.07
2A	21.7	36.05
3	22.0	36.12
4	22.3	35.93
5	22.2	36.08

*Temperature determined using a Yellow Springs Instruments electronic thermometer calibrated against a Hewlett-Packard model 2801 quartz thermometer traceable to the National Bureau of Standards.

**Salinity determined using a model 6230 laboratory salinometer manufactured by Plessey Environmental Systems. All salinities corrected to site bottom temperatures.

7. INTERPRETATION

Laboratory tests indicated that, in homogeneous material of approximately the conductivity of the sediments actually investigated, 90 percent of the volume of material contributing to the conductivity measurements was within the zone extending vertically 56 mm (2.2 in) above and below the probe tips. Thus each measured value of the conductivity reported here represents an average over a vertical range of 110 mm (4.4 in; see sec. 4.1). As the conconductivity of a material decreases, the vertical extent of the zone containing any fixed fraction of the material contributing to the measurement increases. For the materials encountered in this study, the maximum vertical range containing 90 percent of the volume contributing to the measurements is estimated as 0.2 m (8.6 in). In nonhomogeneous materials the current tends to flow in those portions having highest conductivity (Keller and Frischknecht, 1966).

Comparisons among the observed conductivity values as a function of depth, the rates of probe and core penetration, the seismic reflection records, and the field observations of recovered seabed material suggest the following:

(1) The upper portion of the seabed is composed of layers of material, distinguishable by the strength of the seismic reflection signal or by differing conductivity.

(2) The hard reflectors are typically about 0.3 m (1 ft) thick.

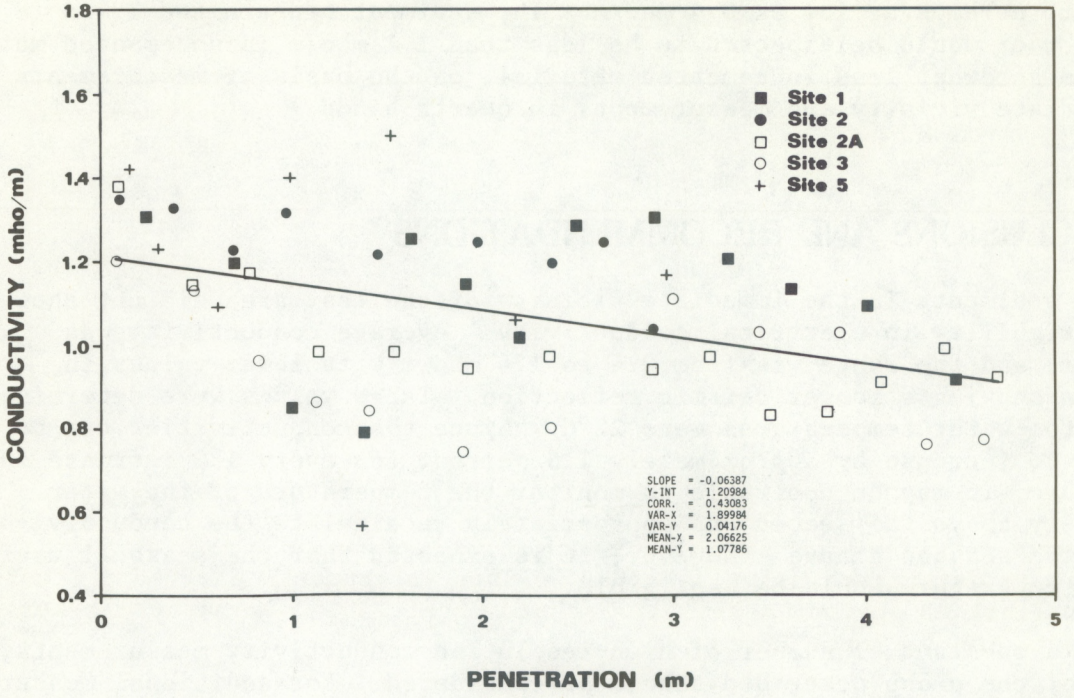

Figure 38.--A composite conductivity regression analysis for five resistivity probe sites in the study area.

(3) Conductivity of the layers giving more intense reflections is approximately 0.5 mho/m, ranging from 0.4 to 0.8 mho/m.

(4) Conductivity of the layers giving weak reflections is typically slightly greater than 1.0 mho/m, ranging from 0.8 to 1.4 mho/m and decreasing slightly with increasing depth of burial.

The layers giving more intense seismic reflections seemed to have greater resistance to penetration by the conductivity probe, probably because of larger coral fragments in these layers. At sites 2 and 3, the probe apparently met penetration refusal with the actual probe tips imbedded in the hard reflector; at site 2A the tips had apparently just broken through the hard reflector at refusal. The conductivity of the sediment in the low area in which the array was located seemed to vary within relatively small limits. The average for the area in the upper 4.9 m (16 ft) was about 1.0 mho/m. Regression analysis of the data suggests an average decrease of 0.061 mho/m per meter below the sea bottom (fig. 38). The low area including site 5 has similar characteristics (see figs. 33-38).

Measurements on the ridge area at site 4 indicate that the lithified material has a relatively high conductivity, approximately the same as the layers giving strong acoustic reflectivity. Because the probe current will flow through the medium of least resistance, in this case the seawater a few centimeters above the probe tips, the conductivities noted at site 4 represent the combined effect of the seawater and the rock. The relatively high final conductivity at site 4 was probably due to the continued operation of the vibrating apparatus and furnished a relatively open current path to the overlying seawater. Rock conductivities at site 4 are believed to be less than

0.7 mho/m, perhaps as low as 0.4 mho/m. The sediment beneath the 2.4 m (8 ft) or so of rock would be expected to be less than 1.1 mho/m in uncemented material, and somewhat less in cemented material, on the basis of measurements in the immediate vicinity and measurements in quartz sands.

8. CONCLUSIONS AND RECOMMENDATIONS

The sediments in the immediate vicinity of the test area did not show great variability in electrical conductivity. Average conductivity was 1.0 mho/m, and the range was from 0.4 to 1.4 mho/m with lower values in materials showing stronger seismic reflection. These values were determined when bottom-water temperatures were 22°C. Since the conductivities can be expected to increase by approximately 1.5 percent for every 1°C increase in temperature, it may be desirable to monitor the temperature of the water immediately above the seabed and appropriately recalculate the conductivities as the seasons change. However, it is expected that the seasonal variation in temperature would be negligible.

For a substantial number of high-resolution conductivity measurements, the use of the probe described should be considered. For additional measurements in coarse or fine-grained sediment at penetration depths up to 5.5 m (18 ft), the system designed and used in this project should again prove satisfactory.

9. REFERENCES

Boyce, R. E., 1967. Electrical resistivity of modern marine sediments from the Bering Sea. NUWC Research Report TP6, 106 pp.

Dobrin, M. B., 1976. Introduction to Geophysical Prospecting, 3rd ed. McGraw-Hill, New York, 630 pp.

Duane, D., and E. Meisburger, 1969. Geomorphology and sediments of the nearshore continental shelf Miami to Palm Beach, Florida. Tech. Memo. No. 29, U.S. Army Corps of Engineers.

Erchul, R. A., 1974. Ocean engineering applications for electrical resistivity techniques. OTC Paper 2012, Offshore Technology Conf., 733-746.

Ginzburg, A., 1974. Resistivity surveying. Geophys. Surv. 1:325-355.

Griffiths, G. V., and R. F. King, 1965. Applied Geophysics. Pergamon Press, Oxford, 223 pp.

Handbook of Marine Science, 1974. F. C. Smith (ed.), Vol. 1, CRC Press, 627 pp.

International Oceanographic Tables, 1966. National Institute of Oceanography of Great Britain and the United Nations Educational Scientific and Cultural Organization.

Jackson, P. D., 1975. An electrical resistivity method for evaluating of the in-situ porosity of clean marine sands. Mar. Geotech. 1:91-115.

Keller, G. V., and F. C. Frischknecht, 1966. Electrical Methods in Geophysical Prospecting. Pergamon Press, New York, 519 pp.

Kermabon, A., C. Gehin, and P. Blauier, 1969. A deep-sea electrical resistivity probe for measuring porosity and density of unconsolidated sediments. Geophysics 34(1):554-571.

Lighty, R. C., I. G. MacIntyre, and R. Stuckenrath, 1978. Submerged early Holocene barrier reef southeast Florida shelf. Nature 276:59-60.

Multer, H. G., and J. E. Hoffmeister, 1968. Subaerial laminated crusts of the Florida Keys. Bull. Geol. Soc. Amer. 79:183-192.

Parkhomenko, E. I., 1967. Electrical Properties of Rocks (translated from Russian by G. V. Keller). Plenum Press, New York, 314 pp.

Pirson, S. J., 1963. Handbook of Well Log Analysis. Prentice-Hall, Inc., Englewood Cliffs, N.J., 326 pp.

Raymond, W. F., 1972. The marine geology of Broward County, Florida. Unpublished Master's thesis, Florida State Univ., 95 pp.

Shinn, E. A., J. H. Hudson, R. B. Halley, and B. Kidz, 1977. Topographic control and accumulation rate of some Holocene coral reefs: South Florida and Dry Tortugas. Proc., III International Coral Reef Symp., Vol. II, Univ. of Miami, Fla., 1-8.

Siegel, V. B., 1959. Reconnaissance survey of the Straits of Florida. Marine Laboratory of the Univ. of Miami, Coral Gables, Fla., TR 59-3.

Strangeway, D. W., 1966. Electromagnetic scale modeling. Methods and Techniques in Geophysics. Vol. 2. S. K. Runcorn (ed.), Interscience Publishers, London, 1-31.

Sweet, W. E., Jr., 1972. Electrical resistivity in unconsolidated sediments. Sea Grant Report TAMU-SG-72-205, Texas A&M Univ., College Station, 142 pp.

Wenner, F., 1915. A method of measuring earth resistivity. Bull. Nat. Bur. Stand. 13:469-478.

Wyllie, M. R. J., 1963. The Fundamentals of Well Log Interpretation, 3rd ed. Academic Press, New York, 238 pp.

Appendix A: Example Conductivity Calculations

OPERATIONS AND CALCULATIONS FOR PROBE CALIBRATIONS

The probe/instrument response was related to actual specific conductivities of the calibration tanks by the methods described here. From these calibrations, values for the in situ conductivities of the sediments were determined.

Step 1. Individual tanks of varying mixtures of freshwater and seawater were used for both the pre- and postcalibration experiments (fig. A-1 and tables A-1 and A-2). The following operations were carried out:

a. From each tank two 1-liter samples were taken for determination of the conductivities using a precision salinometer.

b. Temperature was measured in each of the calibration tanks.

c. Instrument response was determined by immersion of the probe electrodes in each of the calibration tanks.

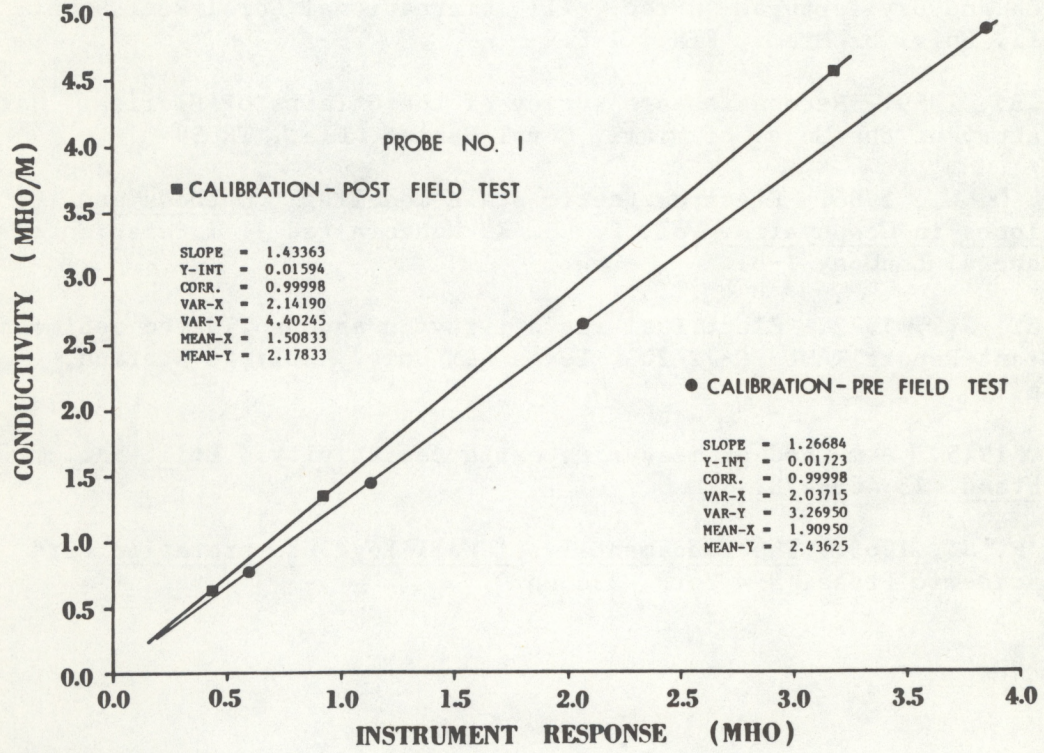

Figure A-1.--Sample calibration data (presented in fig. 11 and repeated here).

Table A-1.--Pre-field-study calibration, probe 1, site 1

Calibration tank number	1	2	3	4
Tank temperature (°C)	22.0	22.5	23.1	23.3
Specific conductivity (mhos/m) of 35°/oo seawater @ tank temperature	4.9954	5.0452	5.1050	5.1250
Conductivity ratio @ tank temperature	0.97756	0.52581	0.28239	0.14961
True specific conductivity (mhos/m) of calibration tank @ tank temperature	4.883	2.653	1.442	0.767
Instrument response V/I (ohms)	0.260	0.484	0.884	1.685
Instrument response I/V (mhos)	3.846	2.067	1.131	0.594

Table A-2.--Post-field-study calibration, probe 1, site 1

Calibration tank number	5	6	7
Tank temperature (°C)	18.3	18.9	19.4
Specific conductivity (mhos/m) of 35°/oo seawater @ tank temperature	4.6268	4.691	4.7364
Conductivity ratio @ tank temperature	0.98670	0.28687	0.13181
True specific conductivity (mhos/m) of calibration tank @ tank temperature	4.565	1.346	0.624
Instrument response V/I (ohms)	0.315	1.091	2.308
Instrument response I/V (mhos)	3.175	0.917	0.433

Step 2. The water samples were analyzed on the Plessey Laboratory salinometer to obtain the ratios of their conductivities to the conductivity of Standard Sea-Water (I.A.P.S.O., Institute of Oceanographic Sciences, Wormley, Godalming, Surrey, England). These conductivity ratios required temperature corrections to relate them to the tank temperatures. Standard correction tables are included in the International Oceanographic Tables, and generally are used to standardize measurements to 15°C or 20°C. In this study, tables were used to interpolate temperature corrections such that conductivity ratios were obtained for a given tank mixture at the tank temperature. It should be noted that the temperature corrections for all calibration tanks were very small, but were made to minimize determinate error. Differences in specific conductivities with and without temperature corrections were calculated to be no greater than 0.5 percent of the observed values.

Table A-3.--Temperature correction*

Conductivity Ratio	Correction ($\times 10^{-5}$)							
	18°	19°	20°	21°	22°	23°	24°	25°
0.10	15	8	0	-7	-15	-22	-29	-36
0.15	21	10	0	-10	-20	-30	-40	-49
0.20	25	12	0	-12	-24	-36	-48	-59
0.25	28	14	0	-14	-27	-41	-54	-67
0.30	31	15	0	-15	-30	-44	-58	-72
0.35	32	16	0	-16	-31	-46	-61	-75
0.40	33	16	0	-16	-32	-47	-62	-77
0.45	33	16	0	-16	-32	-47	-62	-76
0.50	32	16	0	-16	-31	-46	-60	-75
0.55	31	15	0	-15	-30	-44	-58	-72
0.60	29	15	0	-14	-28	-42	-55	-68
0.65	27	13	0	-13	-26	-38	-51	-62
0.70	25	12	0	-12	-23	-35	-46	-56
0.95	5	3	0	-3	-5	-7	-10	-12
0.96	4	2	0	-2	-4	-6	-8	-10
0.97	3	2	0	-2	-3	-4	-6	-7
0.98	2	1	0	-1	-2	-3	-4	-5
0.99	1	1	0	-1	-1	-2	-2	-2
1.00	0	0	0	0	0	0	0	0

*Partial reproduction of International Oceanographic Table IIb.

Note.--This table corrects conductivity ratios to 20°C, but in our study we used it to correct conductivity ratios to calibration tank temperatures.

Example: Postcalibration tank number 5 at 18.3°C

Conductivity ratio obtained from the Plessey Laboratory salinometer = 0.98673 @ 22.8°C (temperature at the time of the salinometer measurement).

From Table IIb in the International Oceanographic Tables, the laboratory-measured conductivity ratio was corrected to the tank temperature. (See partial reproduction of the table in table A-3).

Example:
0.98673 (conductivity ratio @ 22.8°C)
-0.00003 (correction for conductivity ratio from 23°C to 18°C)
0.98670

Step 3. From the Handbook of Marine Science, a plot was constructed relating temperature to specific conductivity of standard seawater @ 35°/oo salinity (conductivity ratio = 1.00000). A linear regression was made with the data and the equation of the relationship obtained (fig. A-2):

$$C = mT + b ,$$

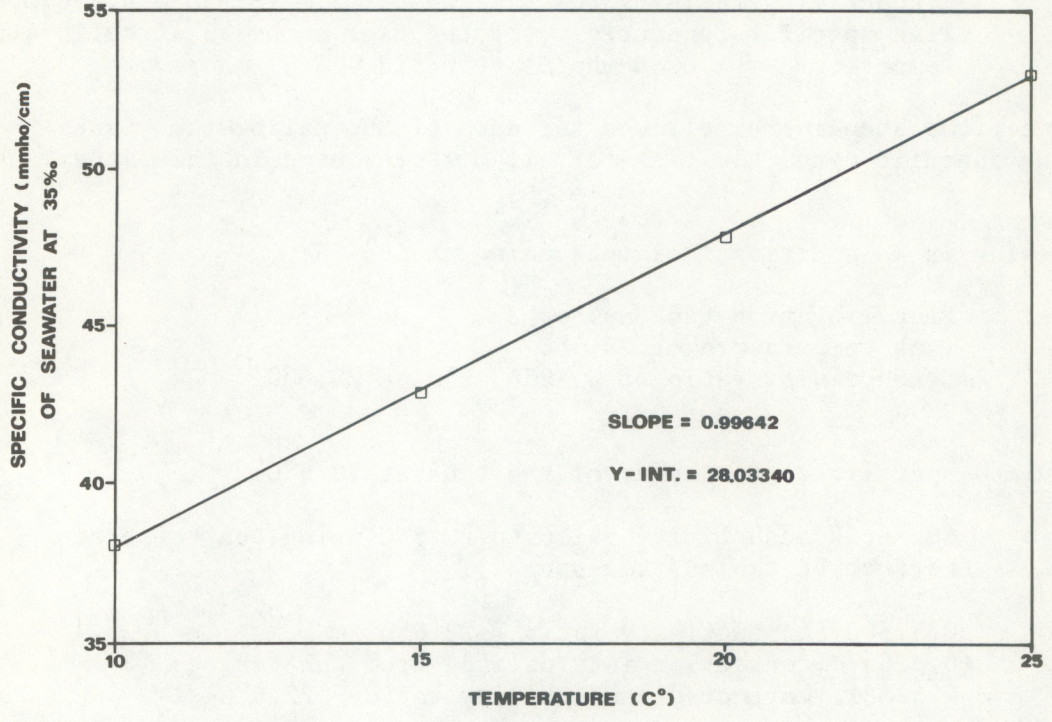

Figure A-2.--A plot relating specific conductivity of seawater at 35°/oo to seawater temperature.

where
C = specific gravity of 35°/oo seawater @ temperature T (mmho/cm)
m = constant (slope) = 0.99642 mmho/cm°C
T = temperature (°C)
b = y-intercept = 28.03340 mmho/cm.

Step 4. Determine the specific conductivity of 35°/oo seawater at the tank temperature. This is derived from the equation in step 3.

Example: Postcalibration tank temperature 18.3°C

Specific conductivity = 0.99642 × 18.3 + 28.03340 of 35°/oo seawater at tank temperature = 46.268 mmho/cm or 4.6268 mho/m.

Note: Conductivity ratio = 1.00000 for 35°/oo seawater.

Step 5. Use the derived data from steps 2 and 4 to obtain true specific conductivity of the tank mixture at the tank temperature. Since the conductivity ratio is a ratio of specific conductivities based on the conductivity of seawater at 35°/oo, a sample analyzed on the salinometer with a salinity of 35°/oo will yield a conductivity ratio of 1.

Given: Specific conductivity of 35°/oo seawater at the tank temperature = 4.6268 mho/m.

Conductivity ratio of the tank number 5 @ 18.3°C = 0.98670.
True specific conductivity of the tank number 5 at calibration temperature = 4.6268 mho/m × 0.98670 = 4.57 mho/m.

The previous steps were followed for each of the calibration tanks to obtain true specific conductivities for all mixtures used in this study.

Following is an additional example using steps 1-5:

Given: Precalibration tank number 2
Tank temperature of 22.5°C
Conductivity ratio of 0.52588 run at 23.0°C

Calculate specific conductivity of the tank at 22.5°C:

a. Correct conductivity ratio to 22.5°C using the temperature correction tables (see step 2):

0.52588 (conductivity ratio @ 23.0°C)
-0.00007 (correction interpolated from the tables)
0.52581 (corrected conductivity ratio @ 22.5°C)

b. Using the equation relating specific conductivity of $35^{o}/oo$ salinity to temperature, determine the specific conductivity of $35^{o}/oo$ salinity at the tank temperature (22.5°C; steps 3 & 4).

Specific conductivity of $35^{o}/oo$ seawater at tank temperature (22.5°C) = 0.99642 × 22.5 + 28.03340 = 50.452 mmho/m or 5.0452 mho/m.

c. Calculate the true specific conductivity of the tank by multiplying the results from (a) by the results from (b):

True specific conductivity of tank number 2 at calibration temperature = 0.52581 × 5.0452 mho/m = 2.653 mho/m.

Appendix B: Resistivity/Conductivity Uncorrected Field Data

Depth (m)	I*	V*	V/I (ohms)**	I/V (mhos)**
SITE 1, PROBE 1				
0.67	23.25	25.02	1.076	0.929
0.98	13.54	20.96	1.548	0.646
1.37	21.23	35.57	1.675	0.597
1.62	26.25	26.92	1.026	0.975
1.89	24.67	27.79	1.126	0.888
2.19	22.16	28.48	1.285	0.778
2.50	25.56	25.48	0.996	1.003
2.90	24.97	24.90	0.997	1.003
3.29	25.12	27.03	1.076	0.929
3.60	27.01	30.95	1.146	0.873
4.02	24.60	29.07	1.182	0.846
4.48	22.48	32.44	1.443	0.693
4.72	20.15	25.24	1.253	0.798
4.79	19.26	21.02	1.091	0.916
SITE 2, PROBE 6				
0.09	17.09	17.58	1.029	0.972
0.37	18.00	18.89	1.049	0.953
0.67	16.74	19.89	1.188	0.842
0.98	16.67	18.38	1.103	0.907
1.46	16.47	19.77	1.200	0.833
1.98	17.63	20.53	1.164	0.859
2.38	16.13	19.65	1.218	0.821
2.65	18.29	21.28	1.163	0.859
2.90	15.39	21.66	1.407	0.711
2.99	13.79	25.15	1.824	0.548
3.02	27.80	65.57	2.359	0.424

*Instrument response.
**Uncorrected by calibrations.

Depth (m)	I*	V*	V/I (ohms)**	I/V (mhos)**
SITE 2A, PROBE 2				
0.09	18.79	20.04	1.067	0.938
0.48	19.94	22.59	1.133	0.883
0.79	12.41	13.55	1.092	0.916
1.16	18.05	24.00	1.330	0.752
1.55	19.83	26.19	1.321	0.757
1.92	18.16	25.08	1.381	0.724
2.38	17.24	22.75	1.320	0.758
2.90	15.86	21.36	1.347	0.742
3.20	17.17	22.18	1.292	0.774
3.51	16.36	24.82	1.517	0.659
3.81	14.57	21.43	1.471	0.680
4.08	15.95	21.35	1.339	0.747
4.42	17.54	21.80	1.243	0.805
4.69	17.16	23.00	1.340	0.746
5.03	14.35	32.51	2.266	0.441
5.09	23.49	34.85	1.484	0.674
SITE 3, PROBE 4				
0.06	21.13	22.56	1.068	0.937
0.49	20.88	23.41	1.121	0.892
0.82	19.10	25.37	1.328	0.753
1.13	18.71	28.62	1.530	0.654
1.40	14.57	23.00	1.579	0.533
1.89	16.05	28.80	1.794	0.557
2.38	16.16	26.74	1.655	0.604
2.99	18.66	22.06	1.182	0.846
3.44	20.88	26.82	1.284	0.779
3.87	19.75	25.42	1.287	0.776
4.33	18.02	31.51	1.749	0.572
4.91	13.62	27.78	2.040	0.490
5.00	14.97	51.96	3.471	0.288

*Instrument response.
**Uncorrected by calibrations.

Depth (m)	I*	V*	V/I (ohms)**	I/V (mhos)**
SITE 4, PROBE 3				
0.09	9.89	15.13	1.530	0.654
0.12	15.10	24.24	1.605	0.623
0.15	24.06	52.81	2.195	0.456
0.15	27.12	39.40	1.453	0.688
SITE 5, PROBE 5				
0.15	22.04	19.59	0.888	1.125
0.30	19.79	20.38	1.030	0.971
0.61	20.77	24.34	0.853	1.172
0.98	22.24	20.07	0.902	1.108
1.37	21.06	44.42	2.109	0.474
1.52	28.08	22.58	0.803	1.245
2.01	31.62	35.55	1.124	0.889
2.99	38.76	29.48	1.025	0.976
3.81	32.74	27.58	0.842	1.187

*Instrument response.
**Uncorrected by calibrations.

Environmental Research LABORATORIES

The mission of the Environmental Research Laboratories (ERL) is to conduct an integrated program of fundamental research, related technology development, and services to improve understanding and prediction of the geophysical environment comprising the oceans and inland waters, the lower and upper atmosphere, the space environment, and the Earth. The following participate in the ERL missions:

AL *Aeronomy Laboratory.* Studies the physics, dynamics, and chemistry of the stratosphere and the surrounding upper and lower atmosphere.

AOML *Atlantic Oceanographic and Meteorological Laboratories.* Study the physical, chemical, biological, and geological characteristics and processes of the ocean waters, the sea floor, and the atmosphere above the ocean, including tropical meteorology such as hurricanes and tropical weather systems.

ARL *Air Resources Laboratories.* Study the diffusion, transport, dissipation, and chemistry of atmospheric pollutants; develop methods of predicting and controlling atmospheric pollution; monitor the global physical environment to detect climatic change.

GFDL *Geophysical Fluid Dynamics Laboratory.* Studies the dynamics of geophysical fluid systems (the atmosphere, the hydrosphere, and the cryosphere) through theoretical analysis and numerical simulation using powerful, high-speed digital computers.

GLERL *Great Lakes Environmental Research Laboratory.* Studies hydrology, waves, currents, lake levels, biological and chemical processes, and lake-air interaction in the Great Lakes and their watersheds; forecasts lake ice conditions.

NSSL *National Severe Storms Laboratory.* Studies severe-storm circulation and dynamics, and develops techniques to detect and predict tornadoes, thunderstorms, and squall lines.

OWRM *Office of Weather Research and Modification.* Conducts a program of basic and applied research to advance the understanding and define the structure of mesoscale phenomena, to improve short-range weather predictions and warnings, and to identify and test hypotheses for beneficially modifying weather processes.

PMEL *Pacific Marine Environmental Laboratory.* Monitors and predicts the physical and biochemical effects of natural events and human activities on the deep-ocean and coastal marine environments of the Pacific region.

PROFS *Prototype Regional Observing and Forecasting Service.* Evaluates and integrates advanced meteorological measurement, forecasting, and communication/dissemination technologies into functional mesoscale weather forecast system designs for transfer to operational agencies such as NWS, NESS, and FAA.

RFC *Research Facilities Center.* Operates instrumented aircraft for environmental research programs; provides scientific measurement tools, logged data, and associated information for meteorological and oceanographic research programs.

SEL *Space Environment Laboratory.* Studies solar-terrestrial physics (interplanetary, magnetospheric, and ionospheric); develops techniques for forecasting solar disturbances; provides real-time monitoring and forecasting of the space environment.

WIM *Weather Modification Program Office.* Plans and coordinates ERL weather modification projects for precipitation enhancement and severe storms mitigation.

WPL *Wave Propagation Laboratory.* Develops, and applies to research and services, new methods for remote sensing of the geophysical environment.

U.S. DEPARTMENT OF COMMERCE
National Oceanic and Atmospheric Administration
BOULDER, COLORADO 80302